

AD-A194 171

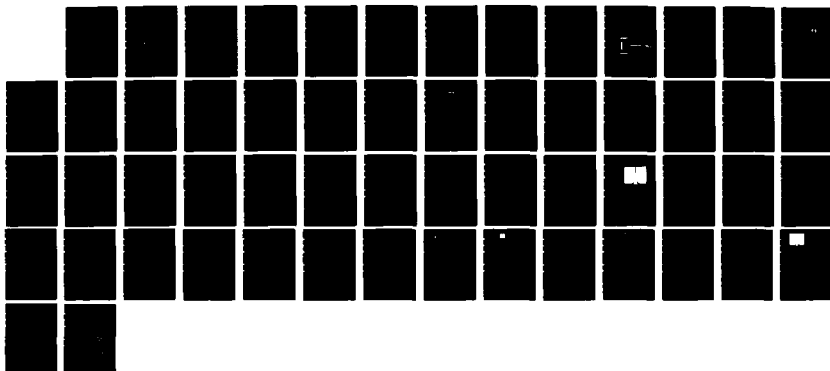
SPECTROSCOPIC STUDIES WITH MULTIPLE QUANTUM WELL
MATERIALS WITH APPLICATIONS (U) TACAN CORP CARLSBAD CA
M M SALOUR 17 NOV 87 ARO-21436 9-EL-5 DAAG29-84-C-0021

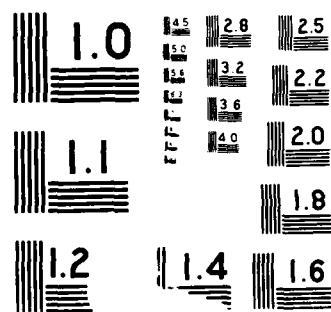
1/1

UNCLASSIFIED

F/G 9/1

NL





AD-A194 171

Spectroscopic Studies With Multiple Quantum Well
Materials With Applications to Optical
Signal Processing at Room Temperature

FINAL REPORT

Dr. Michael M. Salour, Principal Investigator

DTIC
ELECTE
APR 14 1988
S D
ced

17 October 1987

U. S. Army Research Office

#DAAG29-84-C-0021

TACAN Corporation
2111 Palomar Airport Rd.
Carlsbad, CA 92009

APPROVED FOR PUBLIC RELEASE;
DISTRIBUTION UNLIMITED

88 A 11 00N

REPORT DOCUMENTATION PAGE

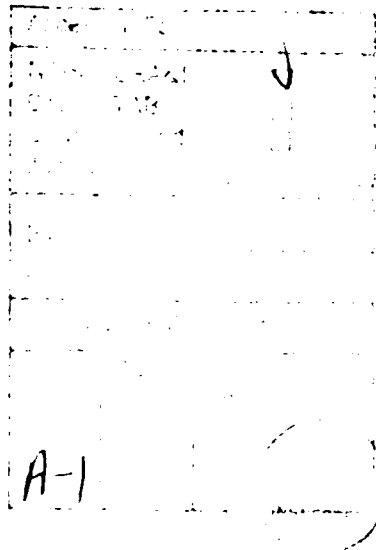
1a. REPORT SECURITY CLASSIFICATION Unclassified		1b. RESTRICTIVE MARKINGS	
2a. SECURITY CLASSIFICATION AUTHORITY		3. DISTRIBUTION/AVAILABILITY OF REPORT Approved for public release; distribution unlimited.	
2b. DECLASSIFICATION/DOWNGRADING SCHEDULE		5. MONITORING ORGANIZATION REPORT NUMBER(S) ARO 21436.9-EL-S	
4. PERFORMING ORGANIZATION REPORT NUMBER(S)		7a. NAME OF MONITORING ORGANIZATION U. S. Army Research Office	
6a. NAME OF PERFORMING ORGANIZATION TACAN Corporation	6b. OFFICE SYMBOL (If applicable)	7b. ADDRESS (City, State, and ZIP Code) P. O. Box 12211 Research Triangle Park, NC 27709-2211	
8a. NAME OF FUNDING/SPONSORING ORGANIZATION U. S. Army Research Office	8b. OFFICE SYMBOL (If applicable)	9. PROCUREMENT INSTRUMENT IDENTIFICATION NUMBER DAAG29-84-C-0021	
10. SOURCE OF FUNDING NUMBERS		11. TITLE (Include Security Classification) Spectroscopic Studies With Multiple Quantum Well Materials With Applications to Optical Signal Processing at Room Temperature	
12. PERSONAL AUTHOR(S) Dr. Michael M. Salour, Principal Investigator		13. TYPE OF REPORT FINAL	
13b. TIME COVERED FROM 17-09-84 TO 17-09-87		14. DATE OF REPORT (Year, Month, Day) 87-11-17	
15. PAGE COUNT 58		16. SUPPLEMENTARY NOTATION The view, opinions and/or findings contained in this report are those of the author(s) and should not be construed as an official Department of the Army position, policy, or decision, unless so designated by other documentation.	
17. COSATI CODES		18. SUBJECT TERMS (Continue on reverse if necessary and identify by block number) Optical Signal Processing for Multiple Quantum Wells	
FIELD	GROUP	SUB-GROUP	
19. ABSTRACT (Continue on reverse if necessary and identify by block number) The Purpose of this program was to investigate the variety of laser induced optical processes in multiple quantum well and other nonlinear waveguide materials. These studies combined both theory and experiment. During the course of this work we demonstrated the first optically pumped mode-locked $\text{Al}_{0.3}\text{Ga}_{0.7}\text{As}/\text{GaAs}$ multiple quantum well (MQW) laser in external cavity. The MQW structure with a total thickness of $5\text{ }\mu\text{m}$ was grown by molecular beam epitaxy on a Si-doped GaAs substrate and was synchronously pumped by a mode-locked Kr^+ laser (82) MGz at 647.1 nm . The MQW laser emitted 10 ps pulses at 8085 \AA with peak powers as high as 6W. The demonstrated MQW laser combines desirable properties of quantum wells with advantages of an external cavity, such as specific band-gap design, high beam quality and the possibility of intracavity tailoring of the laser beam. We have demonstrated the first mode-locked Si-doped bulk GaAs laser tunable over 300 \AA range. Several experiments to measure the third order nonlinear optical susceptibility of MQW and other novel nonlinear materials were successfully completed. In particular, we reported the first measurement of the third order nonlinear optical susceptibility of trans-			
20. DISTRIBUTION/AVAILABILITY OF ABSTRACT <input type="checkbox"/> UNCLASSIFIED/UNLIMITED <input type="checkbox"/> SAME AS RPT <input type="checkbox"/> DTIC USERS		21. ABSTRACT SECURITY CLASSIFICATION Unclassified	
22a. NAME OF RESPONSIBLE INDIVIDUAL		22b. TELEPHONE (Include Area Code)	22c. OFFICE SYMBOL

19. contd.

polyacetylene by third harmonic generation in third films. The measured susceptibility ($3\omega = \omega + \omega + \omega$) = 4×10^{-10} esu which is comparable to the magnitude of the large nonlinear susceptibilities measured in the polydiacetylenes.

During the course of this work we reported on 33x compression of 100 ps mode-locked Kr⁺ laser pulses at 647.1 nm by using a fiber-grating-pair compressor. Pulses with very low wings have been achieved by making use of the nonlinear birefringence effect leading to an intensity dependent state of polarization. The discrimination of the wings took place in the grating compressor which acted as a polarizer.

Finally, we reported on frequency doubling of the 647.1 nm line from a mode-locked Kr⁺ laser in a single-mode fiber with pure Ge-doped core. The harmonic light at 323.5 nm builds up after about 20 minutes of laser irradiation at 647.1 nm. Peak powers as low as 600W were sufficient to prepare the fibers for second-harmonic generation.



FORWARD

The purpose of this program was to investigate the variety of laser induced optical processes in multiple quantum well and other nonlinear waveguide materials. These studies combined both theory and experiment. During the course of this work we demonstrated the first optically pumped mode-locked $\text{Al}_{0.3}\text{Ga}_{0.7}\text{As}/\text{GaAs}$ multiple quantum well (MQW) laser in external cavity. The MQW structure with a total thickness of $5\text{ }\mu\text{m}$ was grown by molecular beam epitaxy on a Si-doped GaAs substrate and was synchronously pumped by a mode-locked Kr^+ laser (82 MGz) at 647.1 nm. The MQW laser emitted 10 ps pulses at 8085\AA with peak powers as high as 6W. The demonstrated MQW laser combines desirable properties of quantum wells with advantages of an external cavity, such as specific band-gap design with high beam quality and the possibility of intracavity tailoring of the laser beam. We also demonstrated the first mode-locked Si-doped bulk GaAs laser tunable over a 300\AA range. Several experiments to measure the third order nonlinear optical susceptibility of MQW and other novel nonlinear materials were successfully completed. In particular, we reported the first measurement of the third order nonlinear optical susceptibility of trans-polyacetylene by third harmonic generation in thin films. The measured susceptibility is $\chi^{(3)}$ ($3\omega = \omega + \omega + \omega$) $= 4 \times 10^{-10}$ esu which is comparable to the magnitude of the large nonlinear susceptibilities measured in the polydiacetylenes.

During the course of this work we reported on 33x compression of 100 ps mode-locked Kr^+ laser pulses at 647.1 nm by using a fiber-grating-pair compressor. Pulses with very low wings have been achieved by making use of the nonlinear birefringence effect leading to an intensity dependent state of polarization. The discrimination of the wings took place in the grating compressor which acted as a polarizer.

Finally, we reported on frequency doubling of the 647.1 nm line from a mode-locked Kr^+ laser in a single-mode fiber with pure Ge-doped core. The harmonic light at 323.5 nm builds up after about 20 minutes of laser irradiation at 647.1 nm. Peak powers as low as 600W were sufficient to prepare the fibers for second-harmonic generation.

TABLE OF CONTENTS

Optical Pumping In Multiple Quantum Well Materials	Page 3
Exciton-Polaritron in GaAs and MQW Materials	Page 12
Optical Pumping in Si-Doped GaAs	Page 15
Nonlinear Optical Effects in Optical Waveguides	Page 22
Optical Pulse Compressions in Optical Waveguides	Page 30
Reprints	Page 40

LIST OF FIGURES

Figure 1	Experimental Setup	Page 5
Figure 2	Laser Spectrum (a) Fluorescence Spectrum (b)	Page 7
Figure 3	Autocorrelation Trace	Page 8
Figure 4	Photon Energy	Page 13
Figure 5	Experimental Setup	Page 16
Figure 6	Fluorescence and Laser Spectrum of Si-Doped GaAs Substrates	Page 18
Figure 7	Laser Spectrum of GaAs Substrate/MQW Side	Page 19
Figure 8	Transmitted Pump Power and Second Harmonic Signal	Page 24
Figure 9	Preparation Time of Fibers for SHG vs. Average Pump Power P_0	Page 25
Figure 10	Experimental Setup	Page 31
Figure 11	Autocorrelation Trace of the Compressed Pulses	Page 33
Figure 12	Spectrum Emitted From the Fiber	Page 35

Optical Pumping in Multiple Quantum Well Materials

Since the demonstration of optically pumped semiconductor lasers with external cavity throughout the visible and near infrared¹⁻⁴ with desirable properties such as tunability, high beam quality and generation of short pulses in mode-locked operation, it became very attractive to apply these techniques to multiple-quantum-well (MQW) structures. The optical properties of $\text{Al}_x\text{Ga}_{1-x}\text{As}/\text{GaAs}$ MQW structures have been studied extensively⁵⁻⁸ showing very strong exciton fluorescence and the multiple sub bands in the GaAs wells due to the quantum confinement of electrons and holes. For many different well sizes and MQW structures made by different production techniques, lasing between the cleaved edges has been achieved by transverse pumping⁹⁻¹⁴. The main advantage of superlattices over other optically pumped semiconductor samples is the possibility to use their very sharp resonances to shift the lasing wavelength from the fundamental band edge of GaAs. Hence, by choosing the width of the GaAs wells and the aluminum content of the barriers, these lasers can be specifically designed and optimized to certain wavelength regions.¹⁴

During the course of this work we reported the first synchronously pumped mode-locked MQW laser with external cavity combining the quantum well properties of laser wavelength design with attractive features such as high output powers, high beam quality and pulses as short as 10 ps. Furthermore, our setup provides the possibility of various modifications of the laser by putting additional optical elements into the cavity.

The multiple quantum well structure used in this experiment was grown by molecular beam epitaxy (MBE) on Si-doped $\langle 100 \rangle$ GaAs substrates. The substrate preparation and growth of the superlattice is made by using standard procedures described elsewhere^{7,8}.

The epitaxial layers consist of 0.5 mm GaAs buffer, a 500Å $\text{Al}_{0.7}\text{Ga}_{0.3}\text{As}$ etch stop layer and a superlattice of 250 periods of 100Å GaAs and 100 Å $\text{Al}_{0.3}\text{Ga}_{0.7}\text{As}$. In contrast to all other reported optically pumped MQW lasers, in our experiment the superlattice is pumped longitudinally. The absorption

length of the 647.1 nm pump light is about $0.5 \mu\text{m}$ at 77K in the GaAs wells and $1.0 \mu\text{m}$ in the $\text{Al}_{0.3}\text{Ga}_{0.7}\text{As}$ barriers^{7,8}. Hence, to provide a sufficient gain length the total MQW layer thickness should exceed $2 \mu\text{m}$. Taking into account additional facts such as possible saturation which increases the absorption length at the high pump intensities needed to get the MQW laser over threshold and to provide enough material for sufficient heatflow from the pumped spot to the heatsink, we decided for a total MQW thickness of $5 \mu\text{m}$. The carriers generated in the barriers by absorbing pump light also contribute to the laser process because they diffuse to the wells with a velocity¹⁵ in the order of 10^7 cm/s where they can form excitons.

A large MQW sample was cut into pieces and some of them were mounted with a transparent cyanoacrylate adhesive on a high reflective sapphire mirror with dielectric coating. Sapphire was used because of its high heat conductivity at low temperatures and the thickness of the glue film was below $5 \mu\text{m}$ keeping this heatflow barrier very small. Other pieces were coated with a 2000Å gold film on the MQW side acting as a high reflective mirror ($R=0.94$ at 800 nm) of the external cavity. These samples were glued on an uncoated sapphire substrate. After polishing the GaAs substrate down to $50 \mu\text{m}$ a couple of circles with about 1 mm diameter were defined photolithographically. The substrate within these circles was then removed by selectively etching it down to the etch stop layer which is practically transparent to the pump and MQW laser light. Instead of removing the whole substrate, the described sample with holes provided the possibility to either pump the MQW or the Si-doped GaAs substrate, whose lasing characteristics have been published recently.⁴

The sapphire mirror with the MQW sample was attached to a copper coldfinger and cooling was provided by liquid nitrogen. The dewar with antireflection-coated windows was mounted on a translation stage, making it possible to find those spots on the sample giving the highest output powers and shortest pulses as well as shifting from the MQW laser to the GaAs laser. A 10x microscope objective (Leitz) was used to focus the pump beam onto the sample and to collect the fluorescence light. An estimation of the lasing spot diameter of $3.5 \mu\text{m}$ was possible by measuring the diameter of the holes burnt

into the samples. The 90 percent transmission of the objective at the laser wavelength is fairly low for intracavity use, but from earlier work⁴ it seems that low spherical aberration is more important than highest transmission.

As a pump source a mode-locked Kr⁺ laser was used, emitting 100 ps pulses at 647.1 nm. Because of the 150 nm spacing between the pump laser and MQW laser, it was possible to pump the MQW laser through its 90 percent output coupler and use a dichroic beamsplitter to separate the two beams as illustrated in Figure 1. The laser and fluorescence spectrum of the MQW was measured with a 1/2m monochromator (Jarrell-Ash) having a resolution of 0.5Å. The temporal width of the pulses was measured by means of background-free autocorrelation. Since autocorrelation is most efficient with linearly polarized beams, a Brewster-plate was inserted into the cavity.

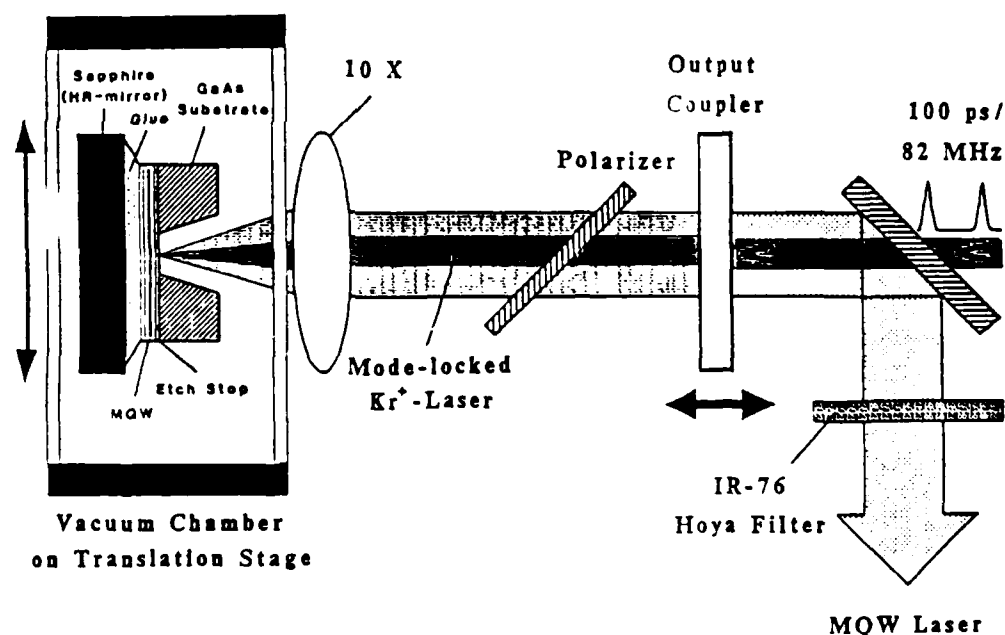


Figure 1. Experimental Setup

Stable average output power as high as 5 mW has been obtained from the MQW laser with 10 percent output coupling and 55 mW pump power. The threshold is around 20 mW, however, it can vary slightly depending on the quality of the lasing spot. The laser power first increases linearly with pump power until it reaches approximately 3x the threshold. For pump powers higher than 60 mW a sharp decrease of the MQW laser power occurs which is most likely due to local heating, enhancing the nonradiative decay of excitons. An increase of the pump power from 50 mW to 70 mW and then decreasing back to 50 mW resulted in about the same output power, proving that the observed power decrease was not caused by permanent damage to the MQW layer. Using the gold coated samples, the highest achievable average power was 3.5 mW and the threshold was 25–30 mW. Scanning the pump beam over the MQW layer resulted in small changes of the laser output indicating a fairly good uniformity of the samples.

Figure 2 shows (a) the MQW laser spectrum and (b) the fluorescence spectrum. Due to the 100Å wells three distinct free exciton transitions can be seen in (b): at 8110Å, at 7870Å and very weakly at 7650Å. The peak at 8320Å is most likely a bound exciton transition.¹⁶ These results are similar to those obtained in Ref. 10 for high pump intensities, however, they can not be compared directly because of the different MQW structures used. Lasing occurs at 8060Å and a second weak line appears at 8300Å. The 240Å spacing between these lines is consistent with the free spectral range (FSR) of the Fabry Perot formed by the 5 mm MQW layer. In contrast to the 10Å mode spacing of the GaAs-laser⁴, the FSR of the thin MQW layer is large enough to achieve single-line operation by cavity alignment only. On the longer wavelength side of the main laserline a second small peak appears 23.5Å apart. The appearance of one or two additional lines, either about 25Å or 36Å separated from the main line, was strongly dependent on the pumped spot. Furthermore, the actual laser wavelength itself could shift from spot to spot giving strong evidence for well size fluctuations. However, since a well size variation of about 3 monolayers of GaAs for 100Å wells can explain the observed lines^{6,16} their relative weakness indicates the high quality of the 250 periods of the MQW structure used. The obtained results are also in good agreement with recently published photoluminescence studies¹⁷ which showed a similar

sensitivity of exciton transitions on well size fluctuations. A better single line operation and more reproducible laser wavelength at a given sample temperature should be obtainable by using 200Å wells because the relative shift of the energy levels of the electrons is less sensitive to well size variations⁶ and only half as many wells are involved.

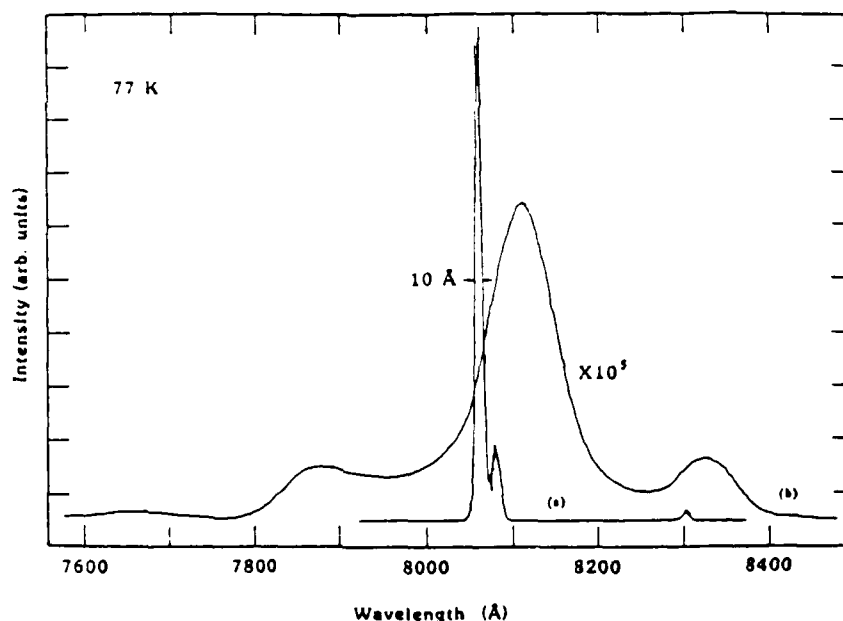


Figure 2. Laser Spectrum (a) Fluorescence Spectrum (b)

An additional effect on the lasing wavelength was caused by the pump beam. Increasing the pump power by 50 mW resulted in a red shift of the laser wavelength of 35Å indicating a severe local heating of the pumped spot. Furthermore, the line broadened by about a factor of 2.7 and additional lines appeared at pump powers higher than 40 mW. To determine the possible temperature tuning range we deliberately let the dewar warm up and observed a shift of the laser wavelength up to 8460Å. A measurement of the temperature was not possible in this experiment because no sensor could be mounted in the dewar used. Together with the results reported on the Si-doped GaAs laser our setup provides a potential tuning range from 8060Å to 8650Å.

The temporal pulsewidth has been measured by background-free autocorrelation. From the shape of the autocorrelation trace shown in Figure 3 we conclude

that single-sided exponential pulses are produced by the MQW laser when tuned to the shortest pulses, which is in agreement with similar results obtained with dye lasers.¹⁸ From the 20 ps width of the autocorrelation trace, the calculated pulse width of the MQW laser is 10 ps. Together with spectral width of 3 Å, the resulting time-bandwidth product is 1.37. The peak power can easily be determined from the average power by multiplication with the inverse duty cycle of 1200, given by the repetition rate and pulse width. Hence, with 5 mW average power, the maximum achievable peak power of our laser is 6 W.

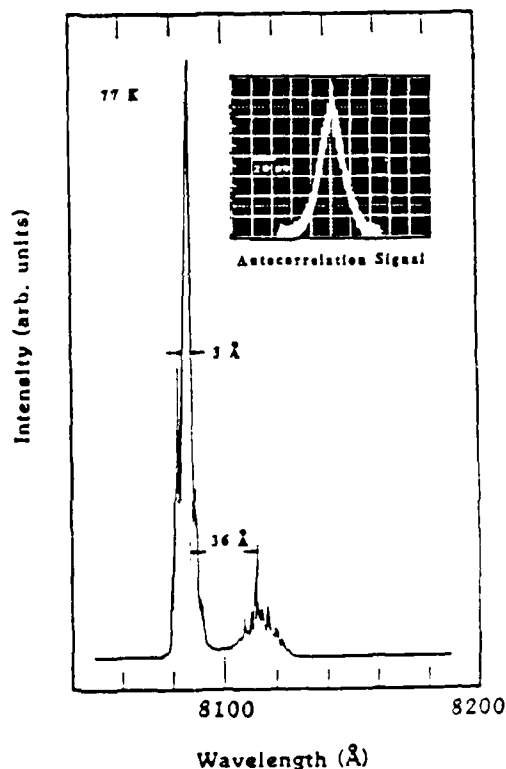


Figure 3. Autocorrelation Trace

This work was the first demonstration of synchronously pumped mode-locked operation of a multiple-quantum-well structure in external cavity. The achieved high output powers are very promising to achieve similar results with other MQW structures such as $\text{Ga}_{0.47}\text{In}_{0.53}\text{As}/\text{Al}_{0.48}\text{In}_{0.52}$ as in which laser already has been reported with cleaved facets at 1.55 μm .¹⁹ Furthermore, the external cavity provides the possibility of further optical intracavity studies.

various MQW structures. The strong sensitivity of the wavelength on the lasing spot can be avoided by using thicker well sizes. However, the emitted wavelength would also shift to longer wavelength. On the other hand one can take advantage of the well size sensitivity by producing wells with steadily increasing size of a few monolayer which should give a very broad fluorescence spectrum. By using a birefringent filter in the cavity, a fairly large tuning range at one temperature can be expected.

Strong and readily saturable MQW excitonic emission has been observed at room temperature,²⁰ therefore, lasing in an external cavity without the need for cryogenic temperatures should be possible by resonant pumping close to the bandgap. Pumping with a commercially available diode laser at room temperature can then lead to an integrated device having major applications in a variety of ultra high speed optical signal processing technologies.

References:

1. C.B. Roxlo and M.M. Salour, Appl. Phys. Lett. 38 738 (1981) .
2. R.S. Putnam, C.B. Roxlo, M.M. Salour, S.H. Groves and M.C. Plonko, Appl. Phys. Lett. 40 660 (1982).
3. R. S. Putnam, M.M. Salour, and T.C. Harman, Appl. Phys. Lett. 43 408 (1983).
4. B. Valk, T.S. Call, M.M. Salour, W. Kopp and H. Morkoc, (to be published in Appl. Phys. Lett. L-7437).
5. D.C. Reynolds, K.K. Bajaj, C.W. Litton, P.W. Yu, J. Klem, C.K. Peng, H. Morkoc, and J. Singh, Appl. Phys. Lett. 48 727 (1986).
6. D.C. Reynolds, K.K. Bajaj, C.W. Litton, P.W. Yu, W.T. Masselink, R. Fischer, and H. Morkoc, Phys. Rev. B 29 7038 (1985).
7. W.T. Masselink, P.J. Pearah, J. Klem, C.K. Peng, H. Morkoc, G.D. Sanders, and Yia-Chung Chang, Phys. Rev. B 32 8027 (1985).
8. P.J. Pearah, W.T. Masselink, J. Klem, T. Henderson, H. Morkoc, C.W. Litton, and D.C. Reynolds, Phys. Rev. B 32 3857 (1985).
9. E.O. Gobel, R. Holger, J. Kuhl, H.J. Polland, and K. Ploog, Appl. Phys. Lett. 47 781 (1985).
10. Z.Y. Xu, V.G. Kreismanis, and C.L. Tang, Appl. Phys. Lett. 43 415 (1983).
11. Z.Y. Xu, V.G. Kreismanis, and C.L. Tang, Appl. Phys. Lett. 44 136 (1984).
12. R.C. Miller, R. Dingle, A.C. Gossard, R. A. Logan, W.A. Nordland, Jr., and W. Wiegmann, J. of Appl. Phys. 47 4509 (1976).

13. J.P. van der Ziel, R. Dingle, R.C. Miller, W. Wiegmann, and W.A. Nordland, Jr., Appl. Phys. Lett. 26 463 (1975).
14. N. Holonyak, Jr., R.M. Kolbas, R.D. Dupuis, and P.D. Dapkus, IEEE QE-16 170 (1980).
15. G.S. Hobson, J. of Physics E: Sci. Inst. 6 229 (1973).
16. D.C. Reynolds - private communication.
17. D.C. Reynolds, K.K. Bajaj, C.W. Litton, J. Singh, P.W. Yu, P. Pearah, J. Klem, and H. Morkoc, Phys. Rev. B 33 5931 (1986).
18. B. Valk, W. Hodel, and H.P. Weber, Opt. Comm. 50 63 (1984).
19. H. Temkin, K. Alavi, W.R. Wagner, T.P. Pearsall, and A.Y. Cho, Appl. Phys. Lett. 42 845 (1983).
20. D.S. Chemla, D.A.B. Miller, P.W. Smith, A.C. Gossard, and W. Wiegman, IEEE QE-20 265 (1984).

Exciton-Polaritron in GaAs and MQW Materials

As a consequence of the coulomb interaction of electron-hole pairs in semiconductors, discrete exciton resonances are created. Their coupling to the light field leads to the concept of the polariton, a mixed exciton-photon state. We have measured a cw absorption spectrum of the GaAs samples, taken with broadband excitation (tungsten lamp) and 0.1-meV resolution (see Figure 1(a)); the $n=1$ and $n=2$ exciton resonances are well resolved. The energetic position of the transverse exciton, $E=1.5151$ eV, is also indicated. Figure 1(b) shows the predicted delay near the $n=1$ exciton-polariton resonance in the single-exciton oscillator model (1), using the values $E=1.5151$ eV, $E_{LT}=0.08$ meV (longitudinal-transverse splitting), $M_{ex}^h = 0.6m_0$ (heavy exciton mass), and $\epsilon_b = 2.6$ (background dielectric constant), known from resonant Brillouin scattering experiments. The temporal delay for pulse propagation on the exciton like lower polariton branch for energies $K_{\omega 0} > E_T + E_{LT}$ is omitted because its contribution to the energy transport is negligible. The dashed line in Figure 1(b) indicates that, in the corresponding energy region, the influence of the $n = 2$ exciton polariton can no longer be neglected.

Polariton dispersion has recently been examined in a number of excitonic systems. Because of the finite effective mass of the exciton in semiconductors, two bulk modes (upper- and lower-branch polaritons) can propagate in the medium when the incident photon energy is higher than the longitudinal exciton energy (E_L). Then the number of the upper- and lower-branch polaritons created at the surface of the crystal must be determined by the Maxwell boundary conditions and the additional boundary conditions (ABC) (2-6). Some experimental methods for the determination of the ABC, such as reflection and resonant Brillouin scattering, have been proposed and carried out. Unfortunately, reflection spectra are usually very sensitive to the character of surface layers (4,7,8) which may exist on the sample. As a result, reflection measurement is not a very sensitive probe of the ABC. Recently, Brillouin scattering efficiency was measured in CdS and compared with some theoretical models (9). A modification of the model proposed independently by several groups (10,11,12) gave results in quantitative agreement with the experiment.

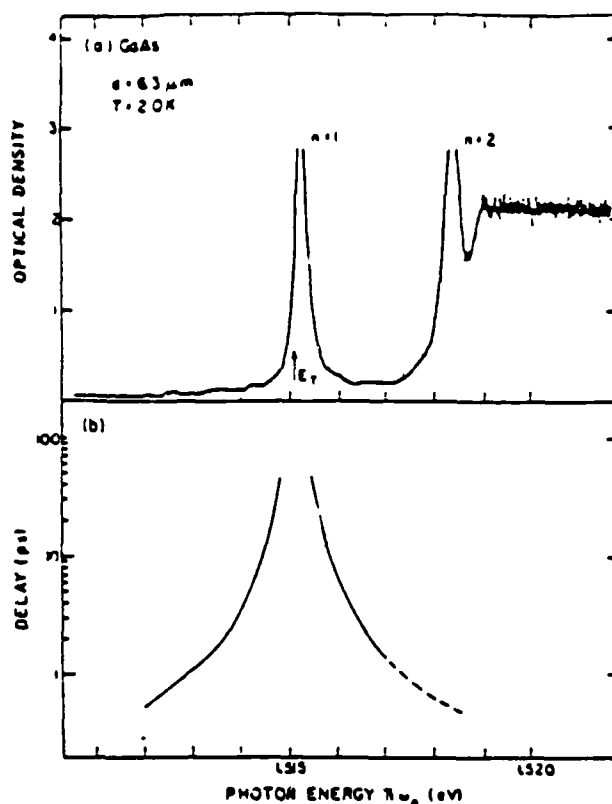


Figure 4. Photon Energy

The optical pumping of the MQW structure leads to the screening of the excitons due to free carriers (created by optical pumping) either directly by interband excitation or indirectly by thermal ionization of optically created excitons. As the excitons are screened, the absorption resonances should saturate, broaden, shift, which, in turn, will give rise to changes in absorption and, consequently, refractive index. With the coupling of the exciton to photon and the concept of polariton, the relative numbers of upper- and lower-branch polaritons can be determined in MQW materials directly by measuring their picosecond induced absorption. The dispersion of the excitonic polariton and the excitonic molecule in MQW can be measured. With the optical excitation of the polariton band, the induced absorption from the polariton to the excitonic molecule should be observable. If the incident photon energy is higher than the longitudinal exciton energy (E_L), then two induced-absorption lines should appear at different photon energies, because of the dispersion of the excitonic molecule. From this induced absorption, the relative numbers of the polaritons of different branches can be determined.

REFERENCES

1. G. W. Fehrenbach and M. M. Salour, Appl. Phys. Lett. 41, 4 (1983).
2. S. I. Pekar, Zh. Eksp. Teor. Fiz. 33, 1022 (1957) [Sov. Phys. JETP 6, 785 (1958)].
3. V. L. Ginzburg, Zh. Eksp. Teor. Fiz. 34, 1593 (1958) [Sov. Phys. JETP 7, 1096 (1958)].
4. J. J. Hopfield and D. G. Thomas, Phys. Rev. 132, 563 (1963).
5. R. Zeyher, J. L. Birman, and W. Brenig, Phys. Rev. B 6, 4613 (1972).
6. A review is given in J. L. Birman, in Excitons, edited by E. I. Rashba and M. D. Sturge (North-Holland, Amsterdam, 1982), Chap. 2.
7. G. D. Mahan and J. J. Hopfield, Phys. Rev. A 135, 428 (1964).
8. F. Evangelisti, A. Frova, and F. Pattela, Phys. Rev. B 10, 4253 (1974).
9. P. Y. Yu and F. Evangelisti, Phys. Rev. Lett. 42, 1642 (1979).
10. J. L. Birman and J. J. Sein, Phys. Rev. B 6, 2482 (1972).
11. G. S. Agarwal, D. N. Pattanayak, and E. Wolf, Phys. Rev. Lett. 27, 1022 (1971), and Phys. Rev. B 10, 1447 (1974).
12. A. A. Maradudin and D. L. Mills, Phys. Rev. B 7, 2787 (1973).

Optical Pumping in Si-Doped GaAs

Optical pumping of semiconductors has the advantage over diode and dye lasers in that virtually any direct-band-gap semiconductor can be used, thereby increasing the available spectral range. Recently mode-locked laser action in external cavity of synchronously pumped semiconductor materials like CdS, CdSe, InGaAsP and HgCdTe has been demonstrated in the wavelength range of 0.49 μm to 2 μm .¹⁻⁵ Mode-locked lasing of thick GaAs bulk crystals has also been observed using a two-photon synchronous pumping configuration.⁶ These lasers have advantages over dye lasers because of the lack of dye instability in the infrared and in addition no jet fluctuations are present, eliminating a very strong source of noise, and they can be operated completely in vacuum. Furthermore, the spontaneous spectrum is narrower than those of dyes, allowing a stabilized single-frequency laser to operate with fewer wavelength selective elements, while tuning can be done by varying the temperature. However, the wavelength range spanning from 0.49 - 2 μm is not yet covered completely by mode-locked semiconductor lasers due to the lack of available high quality semiconductor materials in platelet form of any desired composition.

During the course of this work we reported the development of a cw mode-locked GaAs semiconductor platelet laser whose output frequency and power characteristics provide an attractive tunable source in the near infrared. The laser reported here has the advantage of high beam quality and high output powers compared with other semiconductor lasers operating in the 800 - 900 nm spectral range.⁷

Figure 5 illustrates the experimental setup. A mode-locked Kr^+ laser was used as pump laser emitting 100 ps pulses at 647.1 nm with a repetition rate of 82 MHz and a peak power of 144 W. The pump beam passed: 1) a telescope to compensate for chromatic aberration of the microscope objective, 2) a variable attenuator, 3) a dichroic beamsplitter to separate the GaAs laser beam from the pump beam and 4) the output coupler of the GaAs laser before it was focused onto the GaAs substrate with a 10X microscope objective (Leitz). The pump powers given in the following are always measured in front of the

objective taking into account all losses and the maximum average pump power was 300 mW.

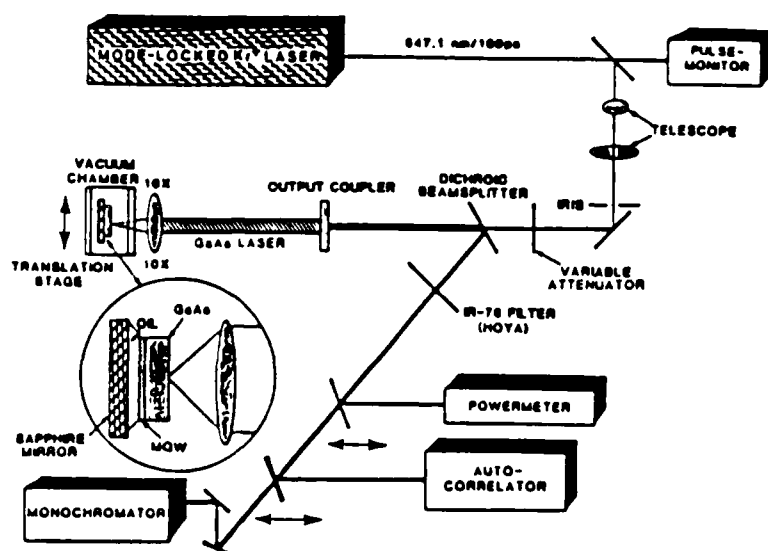


Figure 5. Experimental Setup

The GaAs platelets with a thickness of $100\text{ }\mu\text{m}$ were mounted onto a high reflecting sapphire mirror with a thin film of silicon oil. The GaAs was doped with Si and of a high optical quality, used as substrate to grow Multiple Quantum Well (MQW) superlattices on it.^{8,9} The results reported in this letter have been taken with a sample having a $1\text{ }\mu\text{m}$ MQW layer on its backside. However, we verified spectroscopically that the influence of the MQW on the GaAs laser is negligible because all pump light is absorbed in the substrate before it could reach the MQW layer and the fluorescence light is absorbed by the MQW only below 8300\AA .

The high reflecting mirror with the attached GaAs platelets was mounted on a copper coldfinger of a liquid nitrogen dewar. The dewar itself was sitting on a translation stage for the purpose of alignment and shifting the pumped spot over the sample. The windows of the dewar were coated with a broadband antireflective (AR) coating for the GaAs laser and pump laser. Output

couplers of $R = 0.90$ and $R = 0.97$ were used for our measurements and no tuning or polarizing elements were inserted into the cavity. The GaAs laser output was analyzed by a 1/2m Jarrell Ash monochromator and the pulse width was measured with an autocorrelator. For the temperature tuning of the laser, the dielectric coated sapphire mirror with the platelets was mounted in a cryogenic microminiature refrigeration system (MMR-Technologies K2205) which provided the opportunity to set the temperature between 77K and 300K.

Figure 6 shows (A) the fluorescence spectrum and (B) the laser spectrum. The fluorescence has always been measured with the output coupler removed and is characterized by Fabry Perot modes due to the platelet thickness of about 100 μm and the 30 percent reflectivity at each surface of the substrate. With the $R = 0.90$ output coupler an average laser output of up to 5 mW could be achieved. The laser spectrum (B) usually showed about 7 modes, depending on the excited spot and alignment of the cavity. The linewidth of each mode is 1.5Å (FWHM) and lasing occurred always at the maximum or, due to a lower reabsorption, on the red side of the fluorescence spectrum. We observed that the actual laser wavelength was not only dependent on the temperature of the whole sample but also on the lasing spot itself. Since lasing occurs either on a free or bound exciton transition, the non uniform concentration of impurities in the GaAs sample leads to a wavelength shift by moving from one spot to another. Furthermore, the platelet acts as an intracavity Fabry Perot etalon, tuning the laser to its maximum transmission.

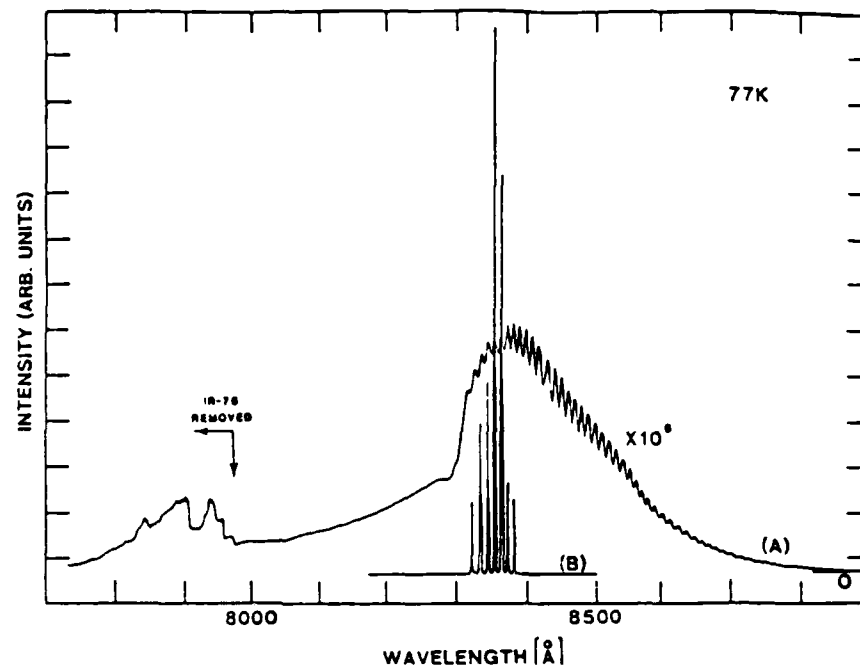


Figure 6. Fluorescence and Laser Spectrum of Si-Doped GaAs Substrate

Figure 7 shows spectra of: (A) GaAs substrate pumped through the MQW layer when lasing, (B) the according fluorescence spectrum, (C) GaAs substrate with MQW structure facing the high reflective mirror, and (D) GaAs substrate with removed MQW (selective etching). Trace (B) shows a strong maximum at 7950\AA due to a strong fluorescence from the MQW layer. Lasing did not occur around this maximum as one might expect but at 8350\AA which is the same wavelength as when pumped through the substrate side (compare Figure 6). Two reasons can explain this result: 1) The luminescence radiation produced within the MQW layer has to penetrate the substrate before it is reflected at the back mirror and light below 8200\AA is reabsorbed by the GaAs substrate, 2) the gain in the MQW layer is not high enough to get the laser over threshold within the layer thickness of $1\text{ }\mu\text{m}$. Pumping a GaAs sample with the MQW structures removed resulted in spectrum (D) without the rapid fluorescence decrease below 8300\AA , which is most likely caused by reabsorption in the MQW layer on the backside of the GaAs platelet [figure 2(A) and 3(C)]. However, no lasing spot could be found on this specific sample.

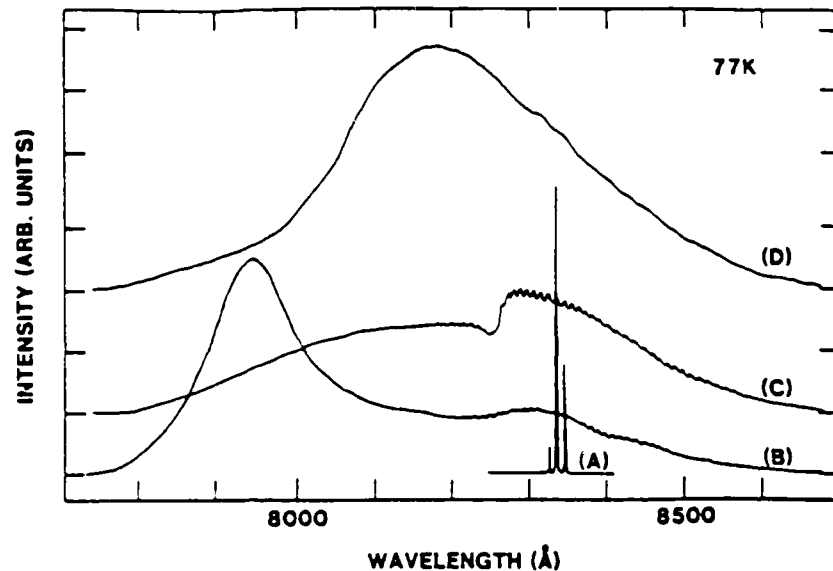


Figure 7. Laser Spectrum of GaAs Substrate/MQW Side

With the $R = 0.90$ output coupler, average powers as high as 5 mW could be achieved with a pump power of 300 mW. The power conversion efficiency is about 1 percent between 1 mW and 5 mW with a $R = 0.90$ output coupler and 0.4 percent when a $R = 0.97$ mirror was used. The threshold pump power was around 120 mW for the 90 percent output couplers and 80 mW for the 97 percent mirror. However, a precise measurement of the threshold was not possible because of its strong dependence on the pumped spot. Furthermore we often found that lasing spots were isolated on the sample such that lasing happened to stop after shifting the sample a few microns. Despite the relatively low efficiency due to the 20 percent intracavity loss of the microscope objective, the achieved powers are much higher than that of other optically pumped GaAs lasers.^{6,11} Using doublet lenses [Melles Griot 06LAI] designed and AR coated for work with diode lasers at 830 nm, failed to achieve any lasing, indicating that a well corrected optical system is more important than using lenses with minimum transmission loss. However, microscope objectives specially designed for intracavity use at the laser wavelength should result in much higher output powers.

The pulsewidth of the laser was determined with an autocorrelator to be 18 ps (FWHM) assuming single-sided exponential pulses. This measurement correlates with the obtained spectral data of the laser linewidth of 1.5\AA , resulting in a time-bandwidth product of 1.16. Thus, the Fabry Perot etalon formed by the GaAs itself reduces the laser bandwidth too much to produce pulses shorter than 10 ps. Using AR coated platelets which removes the etalon effect leads to an increased bandwidth and pulses as short as 7 ps should be achievable.⁶ Additionally, single mode operation as well as fine wavelength tuning with prisms or Lyot filters would be possible.

Wavelength tuning between 8350 and 8650\AA has been accomplished by a controlled setting of the temperature between 77K and 160K. No lasing occurred at temperatures higher than 160K. The observed wavelength shift of about $3\text{\AA}/\text{K}$ is in good agreement with¹¹ but about twice of that found for the CdS lasers.¹

This work demonstrated the first mode-locking of Si doped bulk GaAs platelets producing 18 ps pulses with peak powers of up to 3.3W. AR coating of the crystals may yield a larger intracavity bandwidth and thus even shorter pulses. Furthermore, using GaAs platelets grown by liquid phase epitaxy or similar techniques, having greatly reduced impurity concentration compared to the substrates used, should lead to a better controlled laser wavelength characteristic and cw operation. The GaAs laser fills a gap in the row of synchronously pumped semiconductor lasers in the important wavelength interval between 800 nm and 900 nm. With our pumping scheme a very good beam quality could be achieved which is one of the great advantages over all other GaAs lasers. In addition, other doped semiconductor materials can be used for extended tunable picosecond pulse generation throughout the visible and near infrared.

REFERENCES

1. C.B. Roxlo, D. Bebelaar, and M.M. Salour, Appl. Phys. Lett. **38**, 507 (1981).
2. C.B. Roxlo and M.M. Salour, Appl. Phys. Lett. **38**, 738 (1981).
3. R.S. Putnam, C.B. Roxlo, M.M. Salour, S.H. Groves, and M.C. Plonko, Appl. Phys. Lett. **40**, 660 (1982).
4. R.S. Putnam, M.M. Salour, and T.C. Harman, Appl. Phys. Lett. **43**, 408 (1983).
5. R.S. Putnam and M.M. Salour, Proceedings of the SPIE (Society of Photo-Optical Instrumentation Engineers), Vol. 439, 66 (1984).
6. W.L. Cao, A.M. Vacher, and C.H. Lee, Appl. Phys. Lett. **38**, 653 (1981).
7. J.P. Van der Ziel, Chapter 1 in Semiconductors and Semimetals, Vol. 22, Part B, Lightwave Communications Technology, Ed. W.T. Tsang, Academic Press, Orlando, Florida, 1985.
8. D.C. Reynolds, K. K. Bajaj, C. W. Litton, P.W. Yu, W.T. Masselink, R. Fischer and H. Morkoc, Phys. Rev. B **29**, 7038 (1984).
9. W.T. Masselink, P.J. Pearsall, J. Klem, C.K. Peng, H. Morkoc, G.D. Sanders and Y. C. Chang, Phys. Rev. B **32**, 8027 (1985).
10. S.R. Chinn, J.A. Rossi, C.M. Wolfe, A. Mooradian, IEEE QE-9, 294 (1973).
11. R.C. Miller, R. Dingle, A.C. Gossard, R.A. Logan, W.A. Nordland, and W. Wiegman, J. of Appl. Phys. **47**, 4509 (1976).

Nonlinear Optical Effects in Optical Waveguides

Recently, efficient frequency doubling of the $1.06\text{ }\mu\text{m}$ radiation from mode-locked neodymium:yttrium aluminum garnet (Nd:YAG) lasers in optical fiber has been reported.¹⁻⁵ Since second-order effects in the amorphous core of fibers are normally forbidden, it was necessary to prepare the fibers for efficient second harmonic generation (SHG). They had to be irradiated with high power, Q-switched, and mode-locked pulses from a Nd:YAG laser for ten of hours before SHG could be observed with mode-locked pump pulses only. Using 532 nm harmonic seed pulses along with the $1.06\text{ }\mu\text{m}$ pump light resulted in considerable shortening of the preparation time to only about 5 min. Experiments with different fiber dopants, such as germanium and phosphor, led to the conclusion that phosphorus is a major participant for achieving SHG in fibers.³ Two models have been proposed to describe efficient SHG in optical fibers. One model⁴ postulates color centers as the source of the enhanced second-order nonlinear susceptibility generated by the initially weak second-order susceptibility. The pump and seeded harmonic frequency then mix by third-order nonlinear process to form a dc polarization at the phase-matching periodicity which orients the defects. The fiber thus organizes itself for phase matching and the permanently written periodic nonlinearity leads to efficient SHG within the fiber. A recently published theoretical article⁶ presents a formalism for second harmonic and sum frequency generation in fibers giving estimates for the conversion efficiency due to the non-linear polarization at the core-cladding interface and the bulk nonlinear polarization including quadrupolar terms. A maximum conversion efficiency of about 10^{-5} is predicted under index-matching conditions.

During the course of this program we reported on frequency doubling of the 647.1 nm radiation from a mode-locked Kr^+ laser in a single-mode fiber with purely Ge-doped core. In contrast to the preparation processes described in Refs. 1-3, we observed permanent harmonic generation at 323.5 nm after about 20 min of laser irradiation with peak powers of 720W in the fiber. After the ultraviolet (UV) light started to build up, it reached its maximum value usually within 1-3 min with an average power level on the order of $1\text{ }\mu\text{W}$. The conversion efficiency is on the order of 10^{-6} which is very low compared to

maximum of 5 percent reported for the Nd:YAG laser radiation.³

We also achieved harmonic generation with the Kr^+ laser in a fiber which is single mode at $1.06\text{ }\mu\text{m}$ and bimodal at 647.1 nm . With proper input adjustment, it was possible to excite only the fundamental mode and after 40 min, harmonic light at 323.5 nm was observed. Following this preparation process, 100 ps mode-locked $1.06\text{ }\mu\text{m}$ pulses from a Nd:YAG laser were lanced into the fiber, however, even with average powers of up to 4 W, SHG could not be observed. This result is in agreement with tuning experiments reported in Ref. 4. Before further discussing SHG in fibers, we will first describe the preparation process and the results of several experiments.

The 100 ps pulses at 647.1 nm from a mode-locked Kr^+ laser first passed an acousto-optic modulator (AOM) which isolated the laser from backreflected light, and at the same time, served as a variable attenuator. The maximum average power after the AOM was 820 mW and the light was coupled into the fiber with a 20X microscope objective. The experiments were performed with commercially available single-mode fibers. One fiber [Lightwave Technology (LT) F1506C] had a 7–12 percent Ge-doped silica core of $3.9\text{ }\mu\text{m}$ diameter and a pure silica cladding. A cutoff wavelength of 580 nm , an attenuation of 9.33 dB/km at 633 nm , and a refractive index difference of $\Delta n = 0.4\text{--}0.45\text{ percent}$. The single-mode fiber at $1.06\text{ }\mu\text{m}$ (Corning) had the same doping specifications and index difference but a $5\text{ }\mu\text{m}$ core diameter and a cutoff wavelength of $0.95\text{ }\mu\text{m}$.

The pump and harmonic light emitted from the fiber was collected by means of a 10X objective with 85 percent transmission at 323.5 nm . The UV radiation was measured with a photomultiplier tube (RCA 1P28) after passing several color filters to suppress the remaining pump light. The transmitted pump power P_0 , measured after the 10X output objective, was recorded along with the produced harmonic light and was used as a measure of the power inside the fiber core.

Figure 8 illustrates the time dependence of the preparation process for (a) a 0.8-m-long fiber piece, (b) a 3-m fiber (both F1506C), and (c) a 3-m fiber

piece from Corning. All three fibers were single mode at the pump wavelength. The upper trace shows the transmitted pump light and the lower trace the harmonic light power. After some tens of minutes of irradiation, harmonic light quickly builds up and reaches a first maximum within 1-3 min. The power of the UV radiation is very unstable and oscillates strongly within minutes. These fluctuations are not caused by pump light variations because they are not evident in the smooth upper trace representing the transmitted pump light. Stopping the high power irradiation at a maximum of the harmonic power and then producing SHG at lower pump levels of about 20 mW resulted only in slightly decreased UV intensity fluctuations. The cause of these fluctuations is not clear, but might be overcome by using fibers with additional phosphor doping which could also result in higher conversion efficiencies. For fiber pieces longer than 1m, a sharp decrease in the transmitted pump light was always observed shortly before the harmonic light starts to build up. As shown in Figure 8 (c), this drop in the pump light transmission is more pronounced in the fiber with a smaller core size.

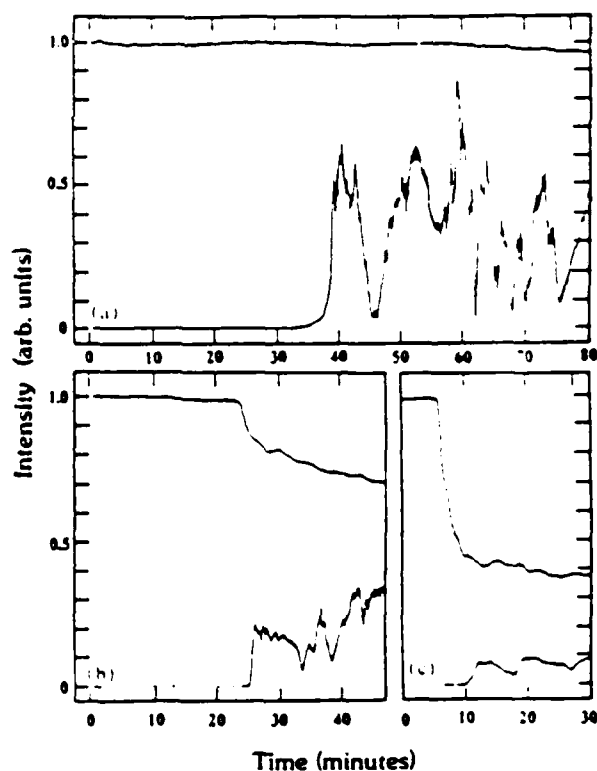


Figure 8. Transmitted Pump Power and Second Harmonic Signal

Although a sharp decline in the transmission was not observed when shorter fiber pieces were prepared, the transmission decreased slowly. Usually after about one hour it stabilized at levels about 3050 percent below the initial value. The described transmission decrease had already been observed earlier, when high power radiation was transmitted through 60-m-long fibers in pulse compression experiments,⁷ and was then attributed to color center generation.

Figure 9 shows the dependence of the required irradiation time to prepare fibers for the second harmonic generation versus pump power. As could be expected, the irradiation time necessary to prepare the fiber for SHG with lower pump powers is longer. The lowest possible average power for a fiber preparation was $P_0 = 450$ mW corresponding to a peak power of about 600W in the core. At average powers P_0 below 400 mW, harmonic light could not be produced even after more than 3h of laser irradiation. The scattering of the data shown in Figure 9 indicates strong variations of the initial conditions for the preparation process. Using seed pulses along with the fundamental should result in more consistent measurements of the preparation time at different power levels.

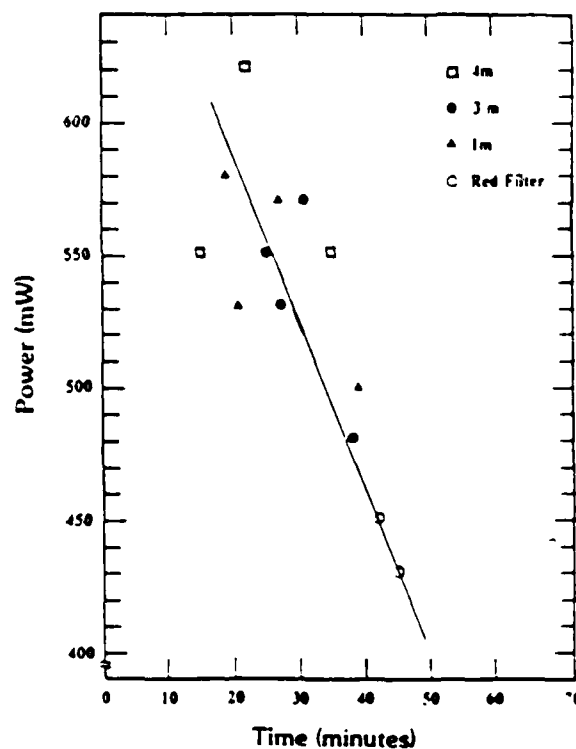


Figure 9. Preparation Time of Fibers for SHG vs. Average Pump Power P_0

By placing a red filter in the pump beam, thereby suppressing wavelengths below 600 nm, we could exclude the possibility of blue and ultraviolet fluorescence light from the Kr^+ laser acting as seed light. The longer time it took to achieve SHG in the fibers is more likely due to the lower pump power, as indicated in Figure 9, than possible seed light suppression. Furthermore, the 20X launch objective used had a very small transmission at the harmonic wavelength, and therefore, experiments with a KDP crystal in the pump beam, producing UV seed pulses, were not successful.

Spectral measurements showed that the linewidth of the harmonic light is $\ll 0.5\text{\AA}$, which was the resolution limit of our spectrometer. A quadratic dependence of the harmonic power could be observed at average pump powers between 20 and 100 mW in the fiber. Due to strong intensity fluctuations, this quadratic dependence was not as apparent at higher pump powers. Polarization measurements basically showed the same results as described in Ref. 3. However, preparation of the fiber with circularly polarized pump light ($P_0 = 500\text{ MW}$) took about 2h and only low harmonic powers could be achieved.

In order to find the optimum fiber length to produce highest harmonic powers, we prepared 3-4-m-long fibers and cut back from the exit end. Due to the strong fluctuations of the harmonic signal, the results of this measurements were very scattered. However, we consistently found that highest harmonic powers were generated with a fiber length between 50 and 70 cm. Lengths shorter than 50 cm always resulted in a decline of the UV signal. This result matches with the walkoff distance estimated for a 100-ps pump pulse and harmonic pulse of the same length using formulas and constants given in Ref. 8.

An estimation of the harmonic power can be made by using the absolute sensitivity of the photomultiplier which has been determined experimentally to be $2.6 \times 10^5\text{ A/W}$ at 355 nm. Knowing the transmission of the filters used, the maximum achieved average power was found to be about $1\text{ }\mu\text{W}$. Another indication of the harmonic power achieved with fibers can be obtained by comparing it with that generated in a crystal. The second harmonic power produced in a 1-mm KDP crystal with an unfocused Gaussian beam of 1.16 mm

width (FWHM) was approximately a factor of 10 less than that obtained with a fiber. Furthermore, with about 600 mW cw pump irradiation, it was possible to obtain continuous harmonic light with an already irradiated fiber prepared for SHG.

Frequency doubling in pure Ge-doped fibers with pump peak powers as low as 600W at 647.1 nm compared to 20 kW necessary at $1.6 \mu\text{m}^1$ strongly supports photoinduced defect or color center generation as the source of the second-order nonlinear susceptibility. Due to a self-organizing effect in the fiber,^{2,4} phase matching is provided and a strong harmonic pulse can develop in the first part of the fiber. Since color centers or defects are easier to produce with shorter wavelengths, it is possible that they are not only generated by the pump light but also by the harmonic pulse within the length of fiber in excess of the walkoff distance. However, a further self-organization of defects to provide phase matching in that part of the fiber cannot be assumed. Additionally, a whole variety of defects is possible in optical fibers^{5,9,14} and therefore, different types of defects may be generated by either the pump or harmonic wavelength. Hence, rather than increasing the harmonic power, such defects may account for the increased attenuation of the pump power which has always been observed.

As pointed out earlier, it was not possible to generate harmonic light with a mode-locked Nd:YAG laser at $1.06 \mu\text{m}$ in a single-mode fiber (@ $1.06 \mu\text{m}$) already prepared for SHG with the Kr^+ laser. We also tuned the Kr^+ laser to the 676.4 nm line and launched powers up to 300 mW in a fiber already prepared for SHG but could not detect any harmonic light. Both results show that SHG in fibers is strongly correlated to the preparation wavelength and are in agreement with tuning experiments reported in Ref. 4. The demonstrated second harmonic generation in optical fibers with relatively low pump peak powers in the visible opens the possibility of generating harmonic light in fibers with mode-locked and cavity-pumped dye lasers. However, limits would be imposed by the UV transmission of the core material and the relatively short walkoff distance for ps pulses.

Under this program we demonstrated second harmonic generation in purely Ge-doped fibers with peak powers as low as 600W at 647.1 nm. The low power needed for the fiber preparation at this wavelength, compared to experiments performed with infrared pulses, gives strong evidence of color center or defect generation in the fiber as source of the second-order nonlinearity. The negative experimental results on harmonic generation with wavelengths other than that used to prepare the fiber for SHG are in agreement with a model and experiments explaining phase matching by a self-written grating inside the fiber core. Our experiments offer the possibility to achieve frequency doubling in fibers with dye lasers. With a UV transmitting 20X objective and harmonic seed pulses, even shorter preparation times and lower pump powers should be possible. Since the pump wavelength lies conveniently in the range of dye lasers, high-resolution tuning experiments can be performed.

References

1. U. Osterberg and W. Margulis, Opt. Lett. 11, 516 (1986).
2. R. H. Stolen and H. W. K. Tom, Digest of the Conference on Lasers and Electro-Optics (CLEO), Baltimore 1987, paper THL2, p.274.
3. U. Osterberg and W. Margulis, Opt. Lett. 12, 57 (1987).
4. M. C. Farries, P. ST. J. Russell, M. E. Fermann, and D. N. Payne, Electron. Lett. 23, 322 (1987).
5. H. Fevrier and J. M. Batriagues, Digest of the XV International Quantum Electronic Conference (IQEC), Baltimore 1987, paper THGG20, p. 150.
6. R. W. Terhune and D. A. Weinberger, J. Opt. Soc. Am. B 4, 661 (1987).
7. B. Valk, K. Vilhelmsson, and M. M. Salour, Appl. Phys. Lett. 50, 656 (1987).
8. M. J. Adams, An Introduction to Optical Waveguides (Wiley, Chichester, New York, Brisbane, Toronto, 1981)pp. 239-250, table 7.3, column 17.
9. G. N. Greaves, J. Non-Cryst. Solids 32, 295 (1979).
10. M. J. Marrone, S. C. Rashleigh, E. J. Friebele, and K. J. Long, Electron. Lett. 20, 193 (1984).
11. G. H. Sigel, Jr. and M. J. Marrone, J. Non-Cryst. Solids 45, 235 (1981).
12. F. L. Galeener, Solid State Comm. 44, 1037 (1982).
13. P. Kaiser, J. Opt. Soc. Am. 64, 475 (1974).
14. E. J. Friebele, D. L. Griscom, and G. H. Sigel, Jr. J. Appl. Phys. 45, 3424 (1974).

Optical Pulse Compressions in Optical Waveguides

Optical pulse compression by means of a single-mode fiber in conjunction with a grating-pair compressor has become a very powerful technique to achieve ultrashort pulses with mode-locked dye lasers.^{1,2} Optical conditions for the application of this method, concerning fiber length and grating separation, are found for initial pulse durations on the order of some picoseconds.³ However, effective pulse compression of relatively long pulses (80–100 ps) has been demonstrated recently with mode-locked Nd:YAG lasers at $1.06\text{ }\mu\text{m}$ ^{4–6} and at $1.32\text{ }\mu\text{m}$.⁷ To our knowledge, the longest reported pulses which have been compressed in the visible region were 33 ps from a mode-locked and frequency-doubled Nd:YAG laser at $0.532\text{ }\mu\text{m}$.⁸

During the course of this program we reported on 33 times compression of mode-locked Kr^+ laser pulses at 647.1 nm from 100 ps down to three ps. Furthermore, by taking advantage of the nonlinear birefringence effect in the fiber in conjunction with the polarization-dependent transmission of the grating pair, we obtained compressed pulses with very low wings. This method of wing reduction has been applied successfully for soliton-like subpicosecond pulses,⁹ for reshaping of three ps pulses,¹⁰ and in conjunction with a pulse compressor generating subpicosecond pulses.¹¹ The phase shift of each polarization, accumulated by the field components along each of the two principal axes of a fiber, is generally different leading to an elliptical output polarization. It can be linearized by means of a quarter-wave plate or Soleil-Babinet compensator. However, at high peak powers, the polarization becomes intensity dependent and is not the same at the peak of the pulse as in the lower intensity wings. With appropriate polarizers, it is therefore possible to separate these wings from the compressed pulse.

The experimental arrangement is shown in Figure 10. A mode-locked Kr^+ laser (Spectra Physics 171) emits 100-ps pulses at 647.1 nm with a repetition rate of 82 MHz. The average power of the laser was 1.2W. An acousto-optic modulator was used as a variable attenuator and to isolate the laser from backreflected light, which was detrimental for the mode locking. With 20X objective the light was coupled into a 60-m-long single-mode fiber (Lightwave

Technology F1506E) having a fused silica core of $3.6\text{ }\mu\text{m}$ diameter. The attenuation of the fiber at 633 nm was 10.8 dB/km and, taking into account all reflection losses as well as a typical coupling efficiency of $\geq 75\text{ percent}$, the overall transmission was 52 percent . at this point we would like to emphasize the importance of using pure silica core fibers for visible light instead of the more easily available germanium doped core fibers. The latter did not withstand the high peak powers over more than a few hours. After that time we observed a strong increase in attenuation which previously has been attributed to the generation of color centers.¹²

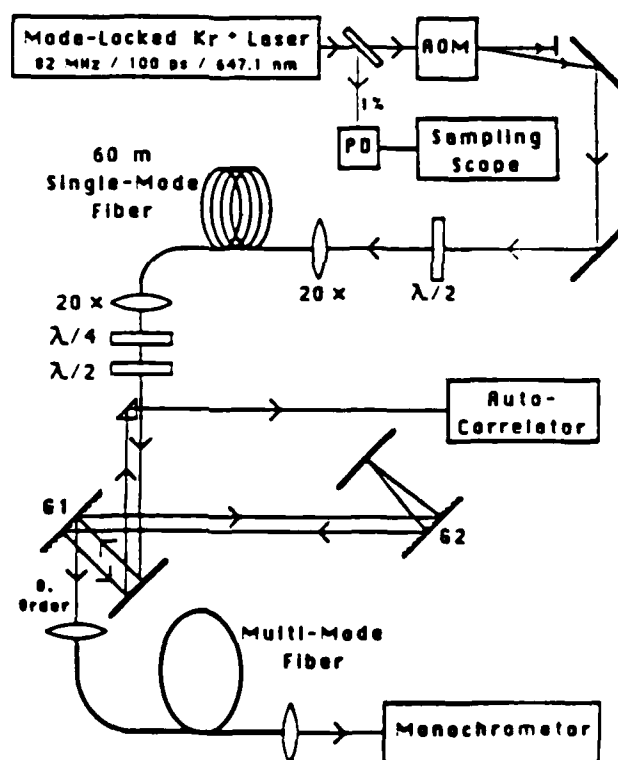


Figure 10. Experimental Setup

With a half-wave plate before the fiber, the orientation of the linear input polarization could be rotated with respect to the principal axes of the fiber. The output polarization could be changed by means of a quarter-wave plate and rotated for maximum transmission through the grating compressor with an additional half-wave plate. The compressor assembly, consisting of two holographic gratings with 2400 1/mm, was used in double-pass configuration producing a round output beam. The gratings were used near Littrow condition with 44° and 57° for the incident and the diffracted beam, respectively. The reflectivity for the s and p polarization was $R_s = 0.65$ and $R_p = 0.1$ (p polarization is parallel to the grooves) resulting in a total double-pass transmission through the grating pair of $T_s = 0.18$ and a negligible transmission for the orthogonal polarization. For compressed pulses of high quality, the typical transmission of the total fiber-grating-pair compressor was about 5 percent. This relatively low transmission can be increased by a factor of 2-3 by using gratings with a higher reflectivity and by operating it in single-pass configuration with appropriate beam-shaping optics.

An autocorrelation trace of the compressed pulses is shown in Figure 11. Assuming a sech^2 shape, the pulse width is 3 ps which corresponds to a compression factor of 33. The average input power was about 1W and the distance between the gratings was 1.88m, corresponding to a compressor length of $b = 3.76\text{m}$. A fine adjustment of the compressor length was not necessary because a slight change of the input power was sufficient to match the peak power in the fiber to the optimal compressor length. The measured average power after the compressor was 47 mW which corresponds to a peak power of about 130W.

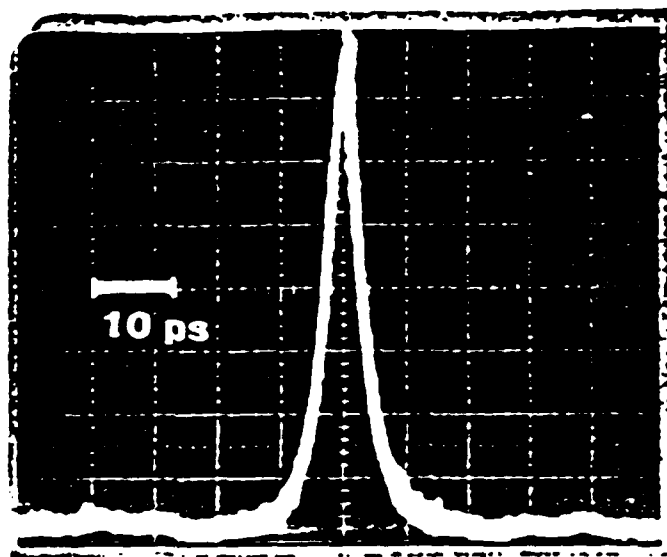


Figure 11. Autocorrelation Trace of the Compressed Pulses

To generate pulses with low wings, as shown in Figure 11, the orientation of the input and output polarization, with respect to the fiber axis and grating pair, was adjusted carefully with the help of the autocorrelation signal. After launching maximum power into the fiber and tuning the half-wave plate after the fiber to maximum transmission through the compressor, rotation of the wave plate at the input and a slight reduction of the input power always resulted in compressed pulses with more or less pronounced wings. Final wing reduction and shortest pulses were then achieved by successively changing the orientation of the input and output half-wave plate along with the quarter-wave plate.¹³ Rotation of the input polarization by 90° together with a readjustment of the wave plates after the fiber resulted in the same pulse shape. At angles between these two orientations, the compressed pulses exhibited various pedestals, wings, and sidelobes or the compression was poor.

In addition to the wing clipping method described above, we tried spectral windowing.¹⁴ It was possible to obtain smooth Gaussian-shaped 7 ps pulses without wings; however, the average power after the compressor dropped to below 1 mW. Therefore, it seems not preferable to use spectral windowing in conjunction with nonpolarization preserving fibers exhibiting nonlinear birefringence.

The spectrum of the pulses after transmission through the fiber is shown in Figure 12. Assuming bandwidth-limited 100-ps Gaussian pulses from the Kr^+ laser, the initial linewidth is 0.0074 nm (FW1/e). The measured width of the spectrum was 0.39 nm corresponding to a spectral broadening by a factor of 53. Additionally, we observed distinct sidelobes in the spectrum (insert Figure 12). Their formation was dependent on the input polarization, and they could be produced repetitively by 45° rotations of the half-wave plate before the fiber. The polarization of the light in the sidelobes was different from that in the central part of the spectrum leading to their suppression in the grating-pair compressor. In a recent paper,¹⁵ such sidelobes were interpreted as optical wave breaking occurring in fibers which are long enough for group velocity dispersion to act on the temporal shape of the pulse. Their generation in our experiment was surprising, since the ratio z/z_0 was about a factor of 10 smaller and the normalized amplitude A larger by a factor of 1.5 than that used for calculations in Ref. 15. A detailed analysis would lie beyond the scope of this letter and is subject to future investigation. In contrast to other pulse compression experiments with long input pulses, we experienced no limitation by stimulated Raman scattering which was always less than 1 percent.

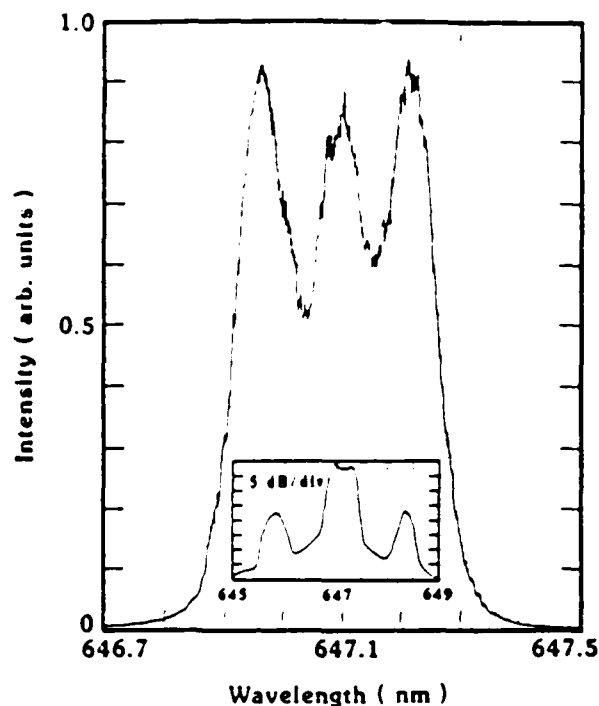


Figure 12. Spectrum Emitted From the Fiber

For a comparison of our results with theory, we use the definitions given in Refs. 3 and 16. For $0.647 \mu\text{m}$ and 100 ps the normalized length is $z_0 = 100 \text{ km}$ ($C_1 = 0.1 \text{ m}^{-1} \text{ ps}^2$). The maximum phase shift $\Delta\phi$ accumulated in a fiber is given by $\Delta\phi = kzn_2I$ with $k = 2\pi/\lambda$ and $n_2 = 3.2 \times 10^{-16} \text{ cm}^2/\text{W}$, z equals the fiber length, and I is the peak intensity. This phase shift is related to the width ω of the broadened spectrum and the initial linewidth $\Delta\omega_{in}$ (both FW1/e) of bandwidth-limited Gaussian pulses by⁹ $\Delta\phi = 1.16 \partial\omega/\Delta\omega_{in}$ and can be determined spectroscopically. $\Delta\phi$ is related to the normalized amplitude A from Ref. 3 by $\Delta\phi = \pi/2 A^2 z/z_0$. Hence, for $z < z_0$, the compression ratio can be expressed by $t_0/t = 1 + 0.57\Delta\phi$ and the grating separation is $b = 0.13\pi C_2 t_0^2/2\Delta\phi$ ($C_2 = 0.133$ for 2400 1/mm and a diffraction angle of 57° , b is in meters and

t_0 is in picoseconds). The 53 times spectral broadening ($\Delta\phi = 61.5$) results in a compression ratio of $t_0/t = 36$ and a grating separation of $b = 4.41\text{m}$, which is in agreement with the experiment. The calculation of the grating separation and the compression ratio with the approach described above led to more reliable values than using the normalized amplitude A estimated from the peak power in the fiber.

Under this program, we have demonstrated the possibility of effectively compressing relatively long pulses with medium peak powers in the visible spectrum to a few picoseconds using a fiber-grating-pair compressor. Additionally, we have demonstrated the feasibility of a pulse-reshaping technique based on the nonlinear birefringence in fibers for long input pulses. A better peak power enhancement can be expected by using gratings with higher reflectivity or by utilizing a single-pass configuration together with beam-shaping optics. One potential application of the compressed pulses is their use as a pump source for optically pumped GaAs multiple quantum well lasers¹⁷ which should lead to the generation of subpicosecond pulses from those lasers.

REFERENCES

1. B. Nikolaus and D. Grischkowski, Appl. Phys. Lett. 42, I (1983); S. L. Palfrey and D. Grischkowski, Opt. Lett. 10, 562 (1985).
2. W. H. Knox, R. L. Fork, M. C. Downer, R. H. Stolen, C. V. Shank, and J. A. Valdmanis, Appl. Phys. Lett. 46 1120 (1985).
3. W. J. Tomlinson, R. H. Stolen, and C. V. Shank, J. Opt. Soc. Am. B1, 139 (1984).
4. J. D. Kafka, B. H. Kolner, T. Baer, and D. M. Bloo, Opt. Lett. 9, 505 (1984).
5. A. S. L. Gomes, U. Osterberg, W. Sibbett, and J. R. Taylor, Opt. Commun. 54, 377 (1985).
6. B. Zysset, W. Hodel, P. Beaud, and H. P. Weber, Opt. Lett. 11, 156 (1986).
7. K. Tai and A. Tomita, Appl. Phys. Lett. 48, 309 (1986).
8. A. M. Johnson, R. H. Stolen, and W. M. Simpson, Appl. Phys. Lett. 44, 729 (1984).
9. R. H. Stolen, J. Botineau, and A. Ashkin, Opt. Lett. 7, 512 (1982).
10. B. Nicloaus, D. Grischkowsky, and A. C. Balant, Opt. Lett. 8, 189 (1983).
11. N. J. Halas and D. Grischkowsky, Appl. Phys. Lett. 48, 823 (1986).
12. R. H. Stolen, in Optical Fiber Telecommunication, edited by S. E. Miller and A. G. Chynoweth (Academic, New York, San Francisco, London, 1979), Chap. 5.
13. With the help of the quarter-wave plate it was possible to increase the

average power after the compressor; however, after best quality compressed pulses were achieved, the wave plate could be removed without changing the amplitude of the autocorrelation signal. This indicates that the additional power contributed mainly to the long, but low power wings.

14. J. P. Heritage, R. N. Thurston, W. J. Tomlinson, A. M. Weiner, and R. H. Stolen, Appl. Phys. Lett. 47, 87 (1985).
15. W. J. Tomlinson, R. H. Stolen, and A. M. Johnson, Optl Lett. 19, 457 (1985).
16. R. H. Stolen, C. V. Shank, and W. J. Tomlinson, in Ultrafast Phenomena IV, edited by D. H. Auston and K. B. Eisental (Springer, Berlin, Heidelberg, New York, Tokyo, 1986), p.46.
17. B. Valk, M. M. Salour, G. Munns, and H. Morkoc, Appl. Phys. Lett. 49, 549 (1986).

REPRINTS

Reprint articles fully or partially supported by this program are included in the following pages:

Second harmonic generation in Ge-doped fibers with a mode-locked Kr⁺ laser

B. Valk, E. M. Kim, and M. M. Salour

TACAN Aerospace Corporation, 2111 Palomar Airport Road, Carlsbad, California 92009

(Received 4 June 1987; accepted for publication 9 July 1987)

We report on frequency doubling of the 647.1 nm line from a mode-locked Kr⁺ laser in a single-mode fiber with pure Ge-doped core. The harmonic light at 323.5 nm builds up after about 20 min of laser irradiation at 647.1 nm. Peak powers as low as 600 W were sufficient to prepare the fibers for second harmonic generation.

Recently, efficient frequency doubling of the 1.06 μm radiation from mode-locked neodymium:yttrium aluminum garnet (Nd:YAG) lasers in optical fibers has been reported.¹⁻³ Since second-order effects in the amorphous core of fibers are normally forbidden, it was necessary to prepare the fibers for efficient second harmonic generation (SHG). They had to be irradiated with high power, Q-switched, and mode-locked pulses from a Nd:YAG laser for tens of hours before SHG could be observed with mode-locked pump pulses only.¹ Using 532 nm harmonic seed pulses along with the 1.06 μm pump light resulted in considerable shortening of the preparation time to only about 5 min.² Experiments with different fiber dopants, such as germanium and phosphor, led to the conclusion that phosphor is a major participant for achieving SHG in fibers.¹ Two models have been proposed to describe efficient SHG in optical fibers. One model¹ postulates color centers as the source of the enhanced second-order nonlinear susceptibility generated by the initially weak second harmonic light from a nonlinear quadrupole susceptibility. The color centers are created periodically along the fiber at spatial locations where the initial green light intensity is highest, i.e., the pump and harmonic light is in phase. This self-written grating automatically provides phase matching between pump and harmonic light. The other model² assumes a photoinduced effect forming the dipole-allowed second-order susceptibility. The pump and seeded harmonic frequency then mix by a third-order nonlinear process to form a dc polarization at the phase-matching periodicity which orients the defects. The fiber thus organizes itself for phase matching and the permanently written periodic nonlinearity leads to efficient SHG within the fiber. A recently published theoretical article⁴ presents a formalism for second harmonic and sum frequency generation in fibers giving estimates for the conversion efficiency due to the nonlinear polarization at the core-cladding interface and the bulk nonlinear polarization including quadrupolar terms. A maximum conversion efficiency of about 10^{-4} is predicted under index-matching conditions.

In this letter we report on frequency doubling of the 647.1 nm radiation from a mode-locked Kr⁺ laser in a single-mode fiber with a purely Ge-doped core. In contrast to the preparation processes described in Refs. 1-3, we observed permanent harmonic generation at 323.5 nm after about 20 min of laser irradiation with peak powers of 720 W in the fiber. After the ultraviolet (UV) light started to build up, it reached its maximum value usually within 1-3 min

with an average power level on the order of 1 μW . The conversion efficiency is on the order of 10^{-6} which is very low compared to a maximum of 5% reported for the Nd:YAG laser radiation.³

We also achieved harmonic generation with the Kr⁺ laser in a fiber which is single mode at 1.06 μm and bimodal at 647.1 nm. With proper input adjustment, it was possible to excite only the fundamental mode and after 40 min, harmonic light at 323.5 nm was observed. Following this preparation process, 100 ps mode-locked 1.06 μm pulses from a Nd:YAG laser were launched into the fiber, however, even with average powers of up to 4 W, SHG could not be observed. This result is in agreement with tuning experiments reported in Ref. 4. Before further discussing SHG in fibers, we will first describe the preparation process and the results of several experiments.

The 100 ps pulses at 647.1 nm from a mode-locked Kr⁺ laser first passed an acousto-optic modulator (AOM) which isolated the laser from backreflected light, and at the same time, served as a variable attenuator. The maximum average power after the AOM was 820 mW and the light was coupled into the fiber with a $20\times$ microscope objective. The experiments were performed with commercially available single-mode fibers. One fiber [Lightwave Technology (LT) F1506C] had a 7-12% Ge-doped silica core of 3.9 μm diameter and a pure silica cladding. A cutoff wavelength of 580 nm, an attenuation of 9.33 dB/km at 633 nm, and a refractive index difference of $\Delta n = 0.303\%$ were specified by the manufacturer. We also tried a similar fiber from Corning Glass Works specifying 5% Ge doping, a 3-3.5 μm core diameter, and $\Delta n = 0.4-0.45\%$. The single-mode fiber at 1.06 μm (Corning) had the same doping specifications and index difference but a 5 μm core diameter and a cutoff wavelength of 0.95 μm .

The pump and harmonic light emitted from the fiber was collected by means of a $10\times$ objective with 85% transmission at 323.5 nm. The UV radiation was measured with a photomultiplier tube (RCA 1P28) after passing several color filters to suppress the remaining pump light. The transmitted pump power P_{tr} , measured after the $10\times$ output objective, was recorded along with the produced harmonic light and was used as a measure of the power inside the fiber core.

Figure 1 illustrates the time dependence of the preparation process for (a) a 0.8-m-long fiber piece, (b) a 3-m fiber (both F1506C), and (c) a 3-m fiber piece from Corning. All

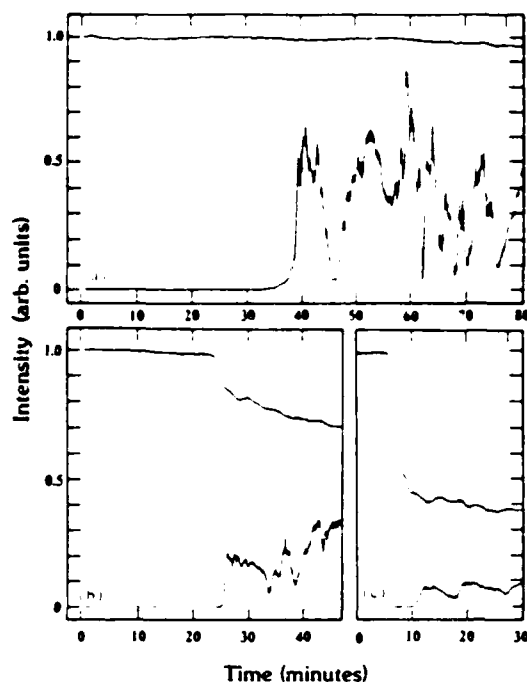


FIG. 1. Transmitted pump power at 647.1 nm (upper trace) and second harmonic signal (lower trace) after (a) 0.8 m fiber (LT) with $P_0 = 500$ mW, (b) 3 m fiber (LT) with $P_0 = 550$ mW, and (c) after 3 m fiber (Corning) with $P_0 = 520$ mW. All fibers were single mode at the pump wavelength and 1 μ W average UV power corresponds to 0.4 units.

three fibers were single mode at the pump wavelength. The upper trace shows the transmitted pump light and the lower trace the harmonic light power. After some tens of minutes of irradiation, harmonic light quickly builds up and reaches a first maximum within 1–3 min. The power of the UV radiation is very unstable and oscillates strongly within minutes. These fluctuations are not caused by pump light variations because they are not evident in the smooth upper trace representing the transmitted pump light. Stopping the high power irradiation at a maximum of the harmonic power and then producing SHG at lower pump levels of about 20 mW resulted only in slightly decreased UV intensity fluctuations. The cause of these fluctuations is not clear, but might be overcome by using fibers with additional phosphor doping which could also result in higher conversion efficiencies. For fiber pieces longer than 1 m a sharp decrease in the transmitted pump light was always observed shortly before the harmonic light starts to build up. As shown in Fig. 1(c), this drop in the pump light transmission is more pronounced in the fiber with a smaller core size. Although a sharp decline in the transmission was not observed when shorter fiber pieces were prepared, the transmission decreased slowly. Usually after about one hour it stabilized at levels about 30–50% below the initial value. The described transmission decrease had already been observed earlier, when high power radiation was transmitted through 60-m-long fibers in pulse compression experiments,⁷ and was then attributed to color center generation.

Figure 2 shows the dependence of the required irradiation time to prepare fibers for the second harmonic generation versus pump power. As could be expected, the irradiation time necessary to prepare the fiber for SHG with lower pump powers is longer. The lowest possible average power for a fiber preparation was $P_0 = 450$ mW corresponding to a peak power of about 600 W in the core. At average powers P_0 below 400 mW, harmonic light could not be produced even after more than 3 h of laser irradiation. The scattering of the data shown in Fig. 2 indicates strong variations of the initial conditions for the preparation process. Using seed pulses along with the fundamental should result in more consistent measurements of the preparation time at different power levels.

By placing a red filter in the pump beam, thereby suppressing wavelengths below 600 nm, we could exclude the possibility of blue and ultraviolet fluorescence light from the Kr^{+} laser acting as seed light. The longer time it took to achieve SHG in the fibers is more likely due to the lower pump power, as indicated in Fig. 2, than possible seed light suppression. Furthermore, the $20\times$ launch objective used had a very small transmission at the harmonic wavelength, and therefore, experiments with a KDP crystal in the pump beam, producing UV seed pulses, were not successful.

Spectral measurements showed that the linewidth of the harmonic light is <0.5 Å, which was the resolution limit of our spectrometer. A quadratic dependence of the harmonic power could be observed at average pump powers between 20 and 100 mW in the fiber. Due to strong intensity fluctuations, this quadratic dependence was not as apparent at higher pump powers. Polarization measurements basically

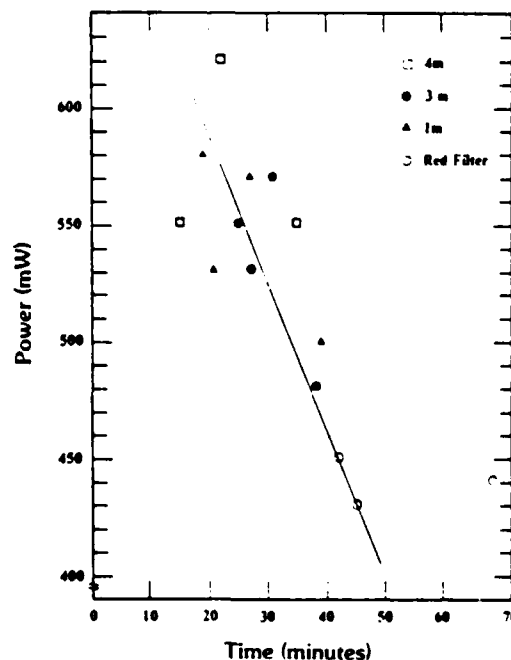


FIG. 2. Preparation time of fibers for SHG vs average pump power P_0 . All data were taken with fiber F1508C. The red filter was placed into the input beam to suppress blue fluorescence light from the Kr^{+} laser.

showed the same results as described in Ref. 3. However, preparation of the fiber with circularly polarized pump light ($P_p = 500$ mW) took about 2 h and only low harmonic powers could be achieved.

In order to find the optimum fiber length to produce highest harmonic powers, we prepared 3–4-m-long fibers and cut back from the exit end. Due to the strong fluctuations of the harmonic signal, the results of this measurement were very scattered. However, we consistently found that highest harmonic powers were generated with a fiber length between 50 and 70 cm. Lengths shorter than 50 cm always resulted in a decline of the UV signal. This result matches with the walkoff distance estimated for a 100-ps pump pulse and harmonic pulse of the same length using formulas and constants given in Ref. 8.

An estimation of the harmonic power can be made by using the absolute sensitivity of the photomultiplier which has been determined experimentally to be 2.6×10^5 A/W at 355 nm. Knowing the transmission of the filters used, the maximum achieved average power was found to be about 1 μ W. Another indication of the harmonic power achieved with fibers can be obtained by comparing it with that generated in a crystal. The second harmonic power produced in a 1-mm KDP crystal with an unfocused Gaussian beam of 1.16 mm width (FWHM) was approximately a factor of 10 less than that obtained with a fiber. Furthermore, with about 600 mW cw pump irradiation it was possible to obtain continuous harmonic light with an already irradiated fiber prepared for SHG.

Frequency doubling in pure Ge-doped fibers with pump peak powers as low as 600 W at 647.1 nm compared to 20 kW necessary at $1.6 \mu\text{m}^2$ strongly supports photoinduced defect or color center generation as the source of the second-order nonlinear susceptibility. Due to a self-organizing effect in the fiber,^{2,4} phase matching is provided and a strong harmonic pulse can develop in the first part of the fiber. Since color centers or defects are easier to produce with shorter wavelengths, it is possible that they are not only generated by the pump light but also by the harmonic pulse within the length of fiber in excess of the walkoff distance. However, a further self-organization of defects to provide phase matching in that part of the fiber cannot be assumed. Additionally, a whole variety of defects is possible in optical fibers^{13–14} and therefore, different types of defects may be generated by either the pump or harmonic wavelength. Hence, rather than increasing the harmonic power, such defects may account for the increased attenuation of the pump power which has always been observed.

As pointed out earlier, it was not possible to generate harmonic light with a mode-locked Nd:YAG laser at $1.06 \mu\text{m}$ in a single-mode fiber ($@ 1.06 \mu\text{m}$) already prepared for SHG with the Kr⁺ laser. We also tuned the Kr⁺ laser to the

676.4 nm line and launched powers up to 300 mW in a fiber already prepared for SHG but could not detect any harmonic light. Both results show that SHG in fibers is strongly correlated to the preparation wavelength and are in agreement with tuning experiments reported in Ref. 4. The demonstrated second harmonic generation in optical fibers with relatively low pump peak powers in the visible opens the possibility of generating harmonic light in fibers with mode-locked and cavity-dumped dye lasers. However, limits would be imposed by the UV transmission of the core material and the relatively short walkoff distance for ps pulses.

In conclusion, we have demonstrated second harmonic generation in purely Ge-doped fibers with peak powers as low as 600 W at 647.1 nm. The low power needed for the fiber preparation at this wavelength, compared to experiments performed with infrared pulses, gives strong evidence of color center or defect generation in the fiber as source of the second-order nonlinearity. The negative experimental results on harmonic generation with wavelengths other than that used to prepare the fiber for SHG are in agreement with a model and experiments explaining phase matching by a self-written grating inside the fiber core. Our experiments offer the possibility to achieve frequency doubling in fibers with dye lasers. With a UV transmitting $20\times$ objective and harmonic seed pulses, even shorter preparation times and lower pump powers should be possible. Since the pump wavelength lies conveniently in the range of dye lasers, high-resolution tuning experiments can be performed.

The authors gratefully acknowledge the technical assistance of R. L. Attaway and discussions with B. Zysset. This work was supported by the U. S. Army Research Office and Rome Air Development Center.

¹U. Osterberg and W. Margulis, *Opt. Lett.* **11**, 516 (1986).

²R. H. Stolen and H. W. K. Tom, *Digest of the Conference on Lasers and Electro-Optics (CLEO)*, Baltimore 1987, paper THL2, p. 274.

³U. Osterberg and W. Margulis, *Opt. Lett.* **12**, 57 (1987).

⁴M. C. Farnes, P. ST. J. Russell, M. E. Fermann, and D. N. Payne, *Electron. Lett.* **23**, 322 (1987).

⁵H. Fevner and J. M. Gabriagues, *Digest of the XV International Quantum Electronic Conference (IQEC)*, Baltimore 1987, paper THGG20, p. 150.

⁶R. W. Terhune and D. A. Weinberger, *J. Opt. Soc. Am.* **B4**, 661 (1987).

⁷B. Valk, K. Vilhelmsen, and M. M. Salour, *Appl. Phys. Lett.* **50**, 656 (1987).

⁸M. J. Adams, *An Introduction to Optical Waveguides* (Wiley, Chichester, New York, Brisbane, Toronto, 1981), pp. 239–250, table 7.3, column 17.

⁹G. N. Greaves, *J. Non-Cryst. Solids* **32**, 295 (1979).

¹⁰M. J. Marrone, S. C. Rashleigh, E. J. Friebele, and K. J. Long, *Electron. Lett.* **20**, 193 (1984).

¹¹G. H. Sigel, Jr. and M. J. Marrone, *J. Non-Cryst. Solids* **45**, 235 (1981).

¹²F. L. Galeener, *Solid State Commun.* **44**, 1037 (1982).

¹³P. Kaiser, *J. Opt. Soc. Am.* **64**, 475 (1974).

¹⁴E. J. Friebele, D. L. Griscom, and G. H. Sigel, Jr., *J. Appl. Phys.* **45**, 3424 (1974).

Optically pumped mode-locked multiple quantum well laser

B. Valk and M. M. Salour

T4CAN Aerospace Corporation, 2111 Palomar Airport Road, Carlsbad, California 92008

G. Munns and H. Morkoç

Coordinated Science Laboratory, University of Illinois, 1101 West Springfield Avenue, Urbana, Illinois 61801

(Received 2 June 1986; accepted for publication 15 July 1986)

We report the first optically pumped mode-locked $\text{Al}_x\text{Ga}_{1-x}\text{As}/\text{GaAs}$ multiple quantum well (MQW) laser in external cavity. The MQW structure with a total thickness of $5\text{ }\mu\text{m}$ was grown by molecular beam epitaxy on a Si-doped GaAs substrate and was synchronously pumped by a mode-locked Kr^+ laser (82 MHz) at 647.1 nm . The MQW laser emitted 10 ps pulses at $8085\text{ }\text{\AA}$ with peak powers as high as 6 W . The demonstrated MQW laser combines desirable properties of quantum wells with advantages of an external cavity, such as specific band-gap design with high beam quality and the possibility of intracavity tailoring of the laser beam.

Since the demonstration of optically pumped semiconductor lasers with external cavity throughout the visible and near infrared¹⁻⁴ with desirable properties such as tunability, high beam quality, and generation of short pulses in mode-locked operation, it became very attractive to apply these techniques to multiple quantum well (MQW) structures. The optical properties of $\text{Al}_x\text{Ga}_{1-x}\text{As}/\text{GaAs}$ MQW structures have been studied extensively⁵⁻⁸ showing very strong exciton fluorescence and the multiple subbands in the GaAs wells due to the quantum confinement of electrons and holes. For many different well sizes and MQW structures made by different production techniques, lasing between the cleaved edges has been achieved by transverse pumping.⁹⁻¹⁴ The main advantage of superlattices over other optically pumped semiconductor samples is the possibility to use their very sharp resonances to shift the lasing wavelength from the fundamental band edge of GaAs. Hence, by choosing the width of the GaAs wells and the aluminum content of the barriers, these lasers can be specifically designed and optimized to certain wavelength regions.¹⁴

In this letter we report the first synchronously pumped mode-locked MQW laser with external cavity combining the quantum well properties of laser wavelength design with attractive features such as high output powers, high beam quality, and pulses as short as 10 ps. Furthermore, our setup provides the possibility of various modifications of the laser by putting additional optical elements into the cavity.

The multiple quantum well structure used in this experiment was grown by molecular beam epitaxy (MBE) on Si-doped (100) GaAs substrates. The substrate preparation and growth of the superlattice are made by using standard procedures described elsewhere.¹⁵ The epitaxial layers consist of $0.5\text{ }\mu\text{m}$ GaAs buffer, a $500\text{ }\text{\AA}$ $\text{Al}_x\text{Ga}_{1-x}\text{As}$ etch stop layer, and a superlattice of 250 periods of $100\text{ }\text{\AA}$ GaAs and $100\text{ }\text{\AA}$ $\text{Al}_x\text{Ga}_{1-x}\text{As}$. In contrast to all other reported optically pumped MQW lasers, in our experiment the superlattice is pumped longitudinally. The absorption length of the 647.1 nm pump light is about $0.5\text{ }\mu\text{m}$ at 77 K in the GaAs wells and $1.0\text{ }\mu\text{m}$ in the $\text{Al}_x\text{Ga}_{1-x}\text{As}$ barriers.¹⁶ Hence, to provide a sufficient gain length the total MQW layer thickness should exceed $2\text{ }\mu\text{m}$. Taking into account additional

facts such as possible saturation which increases the absorption length at the high pump intensities needed to get the MQW laser over threshold and to provide enough material for sufficient heat flow from the pumped spot to the heat-sink, we decided for a total MQW thickness of $5\text{ }\mu\text{m}$. The carriers generated in the barriers by absorbing pump light also contribute to the laser process because they diffuse to the wells with a velocity¹⁷ in the order of 10^7 cm/s where they can form excitons.

A large MQW sample was cut into pieces and some of them were mounted with a transparent cyanoacrylate adhesive on a high reflective sapphire mirror with dielectric coating. Sapphire was used because of its high heat conductivity at low temperatures and the thickness of the glue film was below $5\text{ }\mu\text{m}$ keeping this heat flow barrier very small. Other pieces were coated with a $2000\text{ }\text{\AA}$ gold film on the MQW side acting as a high reflective mirror ($R = 0.94$ at 800 nm) of the external cavity. These samples were glued on an uncoated sapphire substrate. After polishing the GaAs substrate down to $50\text{ }\mu\text{m}$ a couple of circles with about 1 mm diameter were defined photolithographically. The substrate within these circles was then removed by selectively etching it down to the etch stop layer which is practically transparent to the pump and MQW laser light. Instead of removing the whole substrate, the described sample with holes provided the possibility to either pump the MQW or the Si-doped GaAs substrate, whose lasing characteristics have been published recently.⁴

The sapphire mirror with the MQW sample was attached to a copper coldfinger and cooling was provided by liquid nitrogen. The Dewar with antireflection-coated windows was mounted on a translation stage, making it possible to find those spots on the sample giving the highest output powers and shortest pulses as well as shifting from the MQW laser to the GaAs laser. A $10\times$ microscope objective (Leitz) was used to focus the pump beam onto the sample and to collect the fluorescence light. An estimation of the lasing spot diameter of $3.5\text{ }\mu\text{m}$ was possible by measuring the diameter of the holes burnt into the samples. The 90% transmission of the objective at the laser wavelength is fairly low for intracavity use, but from earlier work⁴ it seems that low

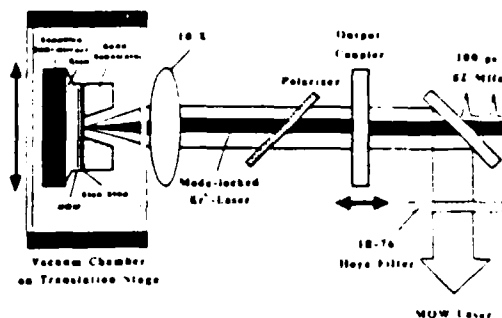


FIG. 1. Experimental setup.

spherical aberration is more important than highest transmission.

As a pump source a mode-locked Kr^+ laser was used, emitting 100 ps pulses at 647.1 nm. Because of the 150 nm spacing between the pump laser and MQW laser, it was possible to pump the MQW laser through its 90% output coupler and use a dichroic beamsplitter to separate the two beams as illustrated in Fig. 1. The laser and fluorescence spectrum of the MQW was measured with a 1/2-m monochromator (Jarrell-Ash) having a resolution of 0.5 Å. The temporal width of the pulses was measured by means of background-free autocorrelation. Since autocorrelation is most efficient with linearly polarized beams, a Brewster plate was inserted into the cavity.

Stable average output power as high as 5 mW has been obtained from the MQW laser with 10% output coupling and 55 mW pump power. The threshold is around 20 mW; however, it can vary slightly depending on the quality of the lasing spot. The laser power first increases linearly with pump power until it reaches approximately $3 \times$ the threshold. For pump powers higher than 60 mW a sharp decrease of the MQW laser power occurs which is most likely due to local heating, enhancing the nonradiative decay of excitons. An increase of the pump power from 50 to 70 mW and then decreasing back to 50 mW resulted in about the same output power, proving that the observed power decrease was not caused by permanent damage to the MQW layer. Using the gold coated samples, the highest achievable average power was 3.5 mW and the threshold was 25–30 mW. Scanning the pump beam over the MQW layer resulted in small changes of the laser output indicating a fairly good uniformity of the samples.

Figure 2 shows (a) the MQW laser spectrum and (b) the fluorescence spectrum. Due to the 100 Å wells three distinct free-exciton transitions can be seen in (b): at 8110 Å, at 7870 Å, and very weakly at 7650 Å. The peak at 8320 Å is most likely a bound exciton transition.¹⁶ These results are similar to those obtained in Ref. 10 for high pump intensities; however, they cannot be compared directly because of the different MQW structures used. Lasing occurs at 8060 Å and a second weak line appears at 8300 Å. The 240 Å spacing between these lines is consistent with the free-spectral range (FSR) of the Fabry-Perot formed by the $5 \mu\text{m}$ MQW layer. In contrast to the 10 Å mode spacing of the GaAs laser,⁴ the

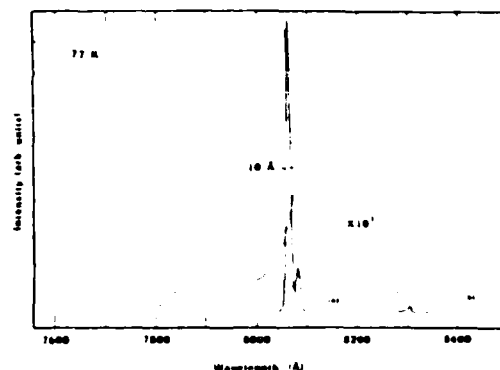


FIG. 2 (a) Laser spectrum (sample with Au coating) and (b) fluorescence spectrum when the output coupler was removed

FSR of the thin MQW layer is large enough to achieve single-line operation by cavity alignment only. On the longer wavelength side of the main laser line a second small peak appears 23.5 Å apart. The appearance of one or two additional lines, either about 25 or 36 Å separated from the main line, was strongly dependent on the pumped spot. Furthermore, the actual laser wavelength itself could shift from spot to spot giving strong evidence for well size fluctuations. However, since a well size variation of about 3 monolayers of GaAs for 100 Å wells can explain the observed lines,^{9,16} their relative weakness indicates the high quality of the 250 periods of the MQW structure used. The obtained results are also in good agreement with recently published photoluminescence studies¹⁷ which showed a similar sensitivity of exciton transitions on well size fluctuations. A better single-line operation and more reproducible laser wavelength at a given sample temperature should be obtainable by using 200 Å wells because the relative shift of the energy levels of the electrons is less sensitive to well size variations⁹ and only half as many wells are involved.

An additional effect on the lasing wavelength was caused by the pump beam. Increasing the pump power by 50 mW resulted in a red shift of the laser wavelength of 35 Å indicating a severe local heating of the pumped spot. Furthermore, the line broadened by about a factor of 2.7 and additional lines appeared at pump powers higher than 40 mW. To determine the possible temperature tuning range we deliberately let the Dewar warm up and observed a shift of the laser wavelength up to 8460 Å. A measurement of the temperature was not possible in this experiment because no sensor could be mounted in the Dewar used. Together with the results reported on the Si-doped GaAs laser our setup provides a potential tuning range from 8060 to 8650 Å.

The temporal pulse width has been measured by background-free autocorrelation. From the shape of the autocorrelation trace shown in Fig. 3 we conclude that single-sided exponential pulses are produced by the MQW laser when tuned to the shortest pulses, which is in agreement with similar results obtained with dye lasers.¹⁸ From the 20 ps width of the autocorrelation trace, the calculated pulse width of the MQW laser is 10 ps. Together with a spectral width of 3 Å, the resulting time-bandwidth product is 1.37. The peak pow-

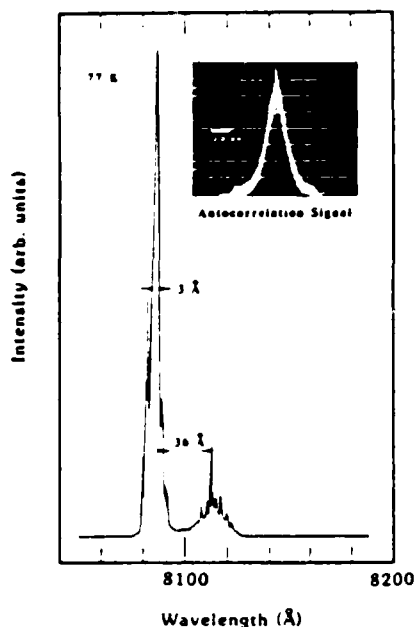


FIG. 3. Autocorrelation trace with a width of 20 ps and the accompanying layer spectrum. The calculated pulse width of the MQW laser is 10 ps and the average output is 4.5 mW.

er can easily be determined from the average power by multiplication with the inverse duty cycle of 1200, given by the repetition rate and pulse width. Hence, with 5 mW average power, the maximum achievable peak power of our laser is 6W.

In conclusion, we have demonstrated synchronously pumped mode-locked operation of a multiple quantum well structure in external cavity. The achieved high output powers are very promising to achieve similar results with other MQW structures such as $\text{Ga}_{0.47}\text{In}_{0.53}\text{As}/\text{Al}_{0.48}\text{In}_{0.52}\text{As}$ in which lasing already has been reported with cleaved facets at $1.55\text{ }\mu\text{m}$.¹⁰ Furthermore, the external cavity provides the possibility of further optical intracavity studies of various MQW structures. The strong sensitivity of the wavelength on the lasing spot can be avoided by using thicker well sizes. However, the emitted laser line would also shift to longer wavelengths. On the other hand, one can take advantage of the well size sensitivity by producing wells with steadily increasing size of a few monolayers which should give a very broad fluorescence spectrum. By using a birefringent filter in

the cavity, a fairly large tuning range at one temperature can be expected.

Strong and readily saturable MQW excitonic emission has been observed at room temperature²¹, therefore, lasing in an external cavity without the need for cryogenic temperatures should be possible by resonant pumping close to the band gap. Pumping with a commercially available diode laser at room temperature can then lead to an integrated device having major applications in a variety of ultrahigh-speed optical signal processing technologies.

The authors gratefully acknowledge helpful discussions with D. C. Reynolds concerning the spectroscopic data, D. Bebelaar for providing a 20-GHz GaAs photodiode, and D. J. Olson and W. Kopp for technical assistance. This work was supported by the U. S. Army Research Office and Air Force Weapons Laboratory. The work done at the Coordinated Science Laboratory was sponsored by the Air Force Office of Scientific Research.

¹C. B. Roxlo and M. M. Salour, *Appl. Phys. Lett.* **38**, 738 (1981).

²R. S. Putnam, C. B. Roxlo, M. M. Salour, S. H. Groves, and M. C. Plonko, *Appl. Phys. Lett.* **40**, 660 (1982).

³R. S. Putnam, M. M. Salour, and T. C. Harman, *Appl. Phys. Lett.* **43**, 408 (1983).

⁴B. Valk, T. S. Call, M. M. Salour, W. Kopp, and H. Morkoç, *Appl. Phys. Lett.* **49**, 119 (1986).

⁵D. C. Reynolds, K. K. Bajaj, C. W. Litton, P. W. Yu, J. Klem, C. K. Peng, H. Morkoç, and J. Singh, *Appl. Phys. Lett.* **48**, 727 (1986).

⁶D. C. Reynolds, K. K. Bajaj, C. W. Litton, P. W. Yu, W. T. Masselink, R. Fischer, and H. Morkoç, *Phys. Rev. B* **29**, 7038 (1985).

⁷W. T. Masselink, P. J. Pearah, J. Klem, C. K. Peng, H. Morkoç, G. D. Sanders, and Yia-Chung Chang, *Phys. Rev. B* **32**, 8027 (1985).

⁸P. J. Pearah, W. T. Masselink, J. Klem, T. Henderson, H. Morkoç, C. W. Litton, and D. C. Reynolds, *Phys. Rev. B* **32**, 3657 (1985).

⁹E. O. Gobel, R. Holger, J. Kuhl, H. J. Pollard, and K. Ploog, *Appl. Phys. Lett.* **47**, 781 (1985).

¹⁰Z. Y. Xu, V. G. Kreismanis, and C. L. Tang, *Appl. Phys. Lett.* **43**, 415 (1983).

¹¹Z. Y. Xu, V. G. Kreismanis, and C. L. Tang, *Appl. Phys. Lett.* **44**, 136 (1984).

¹²R. C. Miller, R. Dingle, A. C. Gossard, R. A. Logan, W. A. Nordland, Jr., and W. Wiegmann, *J. Appl. Phys.* **47**, 4509 (1976).

¹³J. P. van der Ziel, R. Dingle, R. C. Miller, W. Wiegmann, and W. A. Nordland, Jr., *Appl. Phys. Lett.* **26**, 463 (1975).

¹⁴N. Holonyak, Jr., R. M. Kolbas, R. D. Dupuis, and P. D. Dapkus, *IEEE J. Quantum Electron.* **QE-16**, 170 (1980).

¹⁵G. S. Hobson, *J. Phys. E* **6**, 229 (1973).

¹⁶D. C. Reynolds (private communication).

¹⁷D. C. Reynolds, K. K. Bajaj, C. W. Litton, J. Singh, P. W. Yu, P. Pearah, J. Klem, and H. Morkoç, *Phys. Rev. B* **33**, 5931 (1986).

¹⁸B. Valk, W. Hodel, and H. P. Weber, *Opt. Commun.* **50**, 63 (1984).

¹⁹H. Temkin, K. Alavi, W. R. Wagner, T. P. Pearsall, and A. Y. Cho, *Appl. Phys. Lett.* **42**, 845 (1983).

²⁰D. S. Chemla, D. A. B. Miller, P. W. Smith, A. C. Gossard, and W. Wiegmann, *IEEE J. Quantum Electron.* **QE-20**, 265 (1984).

Optically pumped tunable mode-locked Si-doped GaAs laser

B. Valk, T. S. Call, and M. M. Salour

TACAN Aerospace Corporation, 2111 Palomar Airport Road, Carlsbad, California 92008

W. Kopp and H. Morkoç

Coordinated Science Laboratory, University of Illinois, 1101 West Springfield Avenue, Urbana, Illinois 61801

(Received 17 March 1986; accepted for publication 19 May 1986)

Mode-locked operation of Si-doped bulk GaAs in external cavity was achieved by synchronous pumping with a Kr^+ laser at 647.1 nm. High beam quality and peak powers of up to 3.3 W are unique features of this laser. The spontaneous spectrum is narrower than those of dyes, allowing a stabilized single-frequency operation with fewer wavelength selective elements, while tunability over a range of 300 Å was achieved by varying the temperature.

Optical pumping of semiconductors has the advantage over diode and dye lasers in that virtually any direct band-gap semiconductor can be used, thereby increasing the available spectral range. Recently mode-locked laser action in external cavity of synchronously pumped semiconductor materials like CdS, CdSe, InGaAsP, and HgCdTe has been demonstrated in the wavelength range 0.49–2 μm .^{1–5} Mode-locked lasing of thick GaAs bulk crystals has also been observed using a two-photon synchronous pumping configuration.⁶ These lasers have advantages over dye lasers because of the lack of dye instability in the infrared and in addition no jet fluctuations are present, eliminating a very strong source of noise, and they can be operated completely in vacuum. Furthermore, the spontaneous spectrum is narrower than those of dyes, allowing a stabilized single-frequency laser to operate with fewer wavelength selective elements, while tuning can be done by varying the temperature. However, the wavelength range spanning from 0.49 to 2 μm is not yet covered completely by mode-locked semiconductor lasers due to the lack of available high quality semiconductor materials in platelet form of any desired composition.

In this letter we report the development of a cw mode-locked GaAs semiconductor platelet laser whose output frequency and power characteristics provide an attractive tunable source in the near infrared. The laser reported here has the advantage of high beam quality and high output powers compared with other semiconductor lasers operating in the 800–900 nm spectral range.⁷

Figure 1 illustrates the experimental setup. A mode-locked Kr^+ laser was used as pump laser emitting 100 ps pulses at 647.1 nm with a repetition rate of 82 MHz and a peak power of 144 W. The pump beam passed (1) a telescope to compensate for chromatic aberration of the microscope objective, (2) a variable attenuator, (3) a dichroic beamsplitter to separate the GaAs laser beam from the pump beam, and (4) the output coupler of the GaAs laser before it was focused onto the GaAs substrate with a 10 \times microscope objective (Leitz). The pump powers given in the following are always measured in front of the objective taking into account all losses and the maximum average pump power was 300 mW.

The GaAs platelets with a thickness of 100 μm were mounted onto a high reflecting sapphire mirror with a thin film of silicon oil. The GaAs was doped with Si and of a high

optical quality, used as substrate to grow multiple quantum well (MQW) superlattices on it.^{8,9} The results reported in this letter have been taken with a sample having a 1 μm MQW layer on its backside. However, we verified spectroscopically that the influence of the MQW on the GaAs laser is negligible because all pump light is absorbed in the substrate before it could reach the MQW layer and the fluorescence light is absorbed by the MQW only below 8300 Å.

The high reflecting mirror with the attached GaAs platelets was mounted on a copper coldfinger of a liquid nitrogen dewar. The dewar itself was sitting on a translation stage for the purpose of alignment and shifting the pumped spot over the sample. The windows of the dewar were coated with a broadband antireflective (AR) coating for the GaAs laser and pump laser. Output couplers of $R = 0.90$ and $R = 0.97$ were used for our measurements and no tuning or polarizing elements were inserted into the cavity. The GaAs laser output was analyzed by a 1/2-m Jarrell-Ash monochromator and the pulse width was measured with an autocorrelator. For the temperature tuning of the laser, the dielectric coated sapphire mirror with the platelets was mounted in a cryogenic microminiature refrigeration system (MMR-Technologies K2205) which provided the opportunity to set the temperature between 77 and 300 K.

Figure 2 shows (a) the fluorescence spectrum and (b) the laser spectrum. The fluorescence has always been measured with the output coupler removed and is characterized by Fabry-Perot modes due to the platelet thickness of about 100 μm and the 30% reflectivity at each surface of the substrate. With the $R = 0.90$ output coupler an average laser output of up to 5 mW could be achieved. The laser spectrum (b) usually showed about seven modes, depending on the excited spot and alignment of the cavity. The linewidth of each mode is 1.5 Å (FWHM) and lasing occurred always at the maximum or, due to a lower reabsorption, on the red side of the fluorescence spectrum. We observed that the actual laser wavelength was not only dependent on the temperature of the whole sample but also on the lasing spot itself. Since lasing occurs either on a free or bound exciton transition, the nonuniform concentration of impurities in the GaAs sample leads to a wavelength shift by moving from one spot to another. Furthermore, the platelet acts as an intracavity Fabry-Perot étalon, tuning the laser to its maximum transmission.

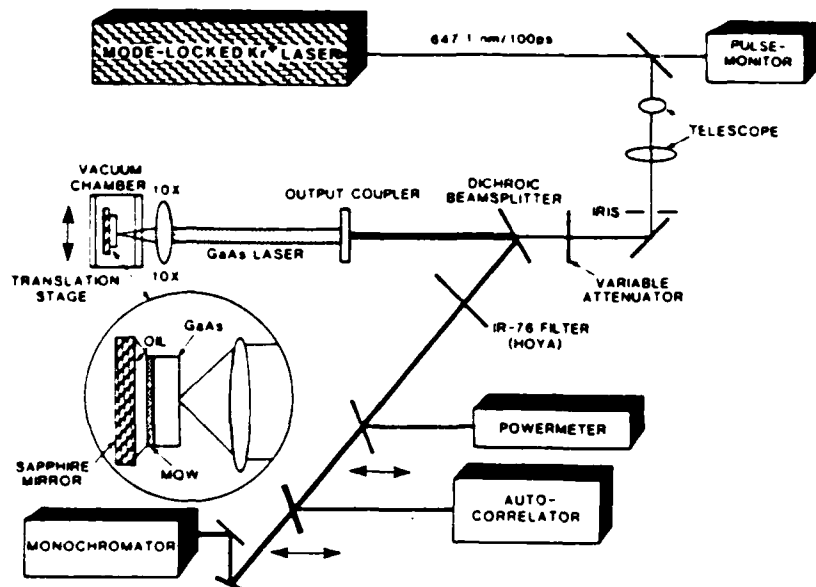


FIG. 1 Experimental setup. IR-76 is a sharp cut filter transmitting at wavelengths longer than 760 nm.

Figure 3 shows spectra of (a) GaAs substrate pumped through the MQW layer when lasing, (b) the corresponding fluorescence spectrum, (c) GaAs substrate with MQW structure facing the high reflective mirror, and (d) GaAs substrate with removed MQW (selective etching). Trace (b) shows a strong maximum at 7950 Å due to a strong fluorescence from the MQW layer. Lasing did not occur around this maximum as one might expect but at 8350 Å which is the same wavelength as when pumped through the substrate side (compare Fig. 2). Two reasons can explain this result: (1) The luminescence radiation produced within the MQW layer has to penetrate the substrate before it is

reflected at the back mirror and light below 8200 Å is reabsorbed by the GaAs substrate; (2) the gain in the MQW layer is not high enough to get the laser over threshold within the layer thickness of 1 µm. Pumping a GaAs sample with the MQW structures removed resulted in spectrum (d) without the rapid fluorescence decrease below 8300 Å, which is most likely caused by reabsorption in the MQW layer on the backside of the GaAs platelet [Figs. 2(a) and 3(c)]. However, no lasing spot could be found on this specific sample.

With the $R = 0.90$ output coupler, average powers as high as 5 mW could be achieved with a pump power of 300

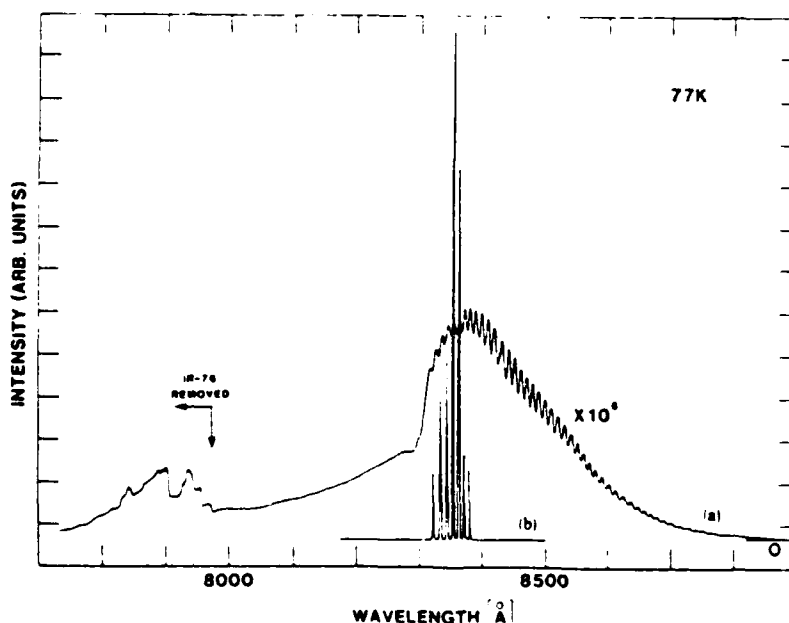


FIG. 2. Fluorescence and laser spectrum of a Si-doped GaAs substrate (MQW layer facing high reflective mirror): (a) Fluorescence spectrum measured with the output coupler removed and a 10^6 times higher sensitivity compared to (b) the laser spectrum. The latter was obtained with a 90% output coupler and 380 mW average pump power resulting in 3 mW GaAs laser power.

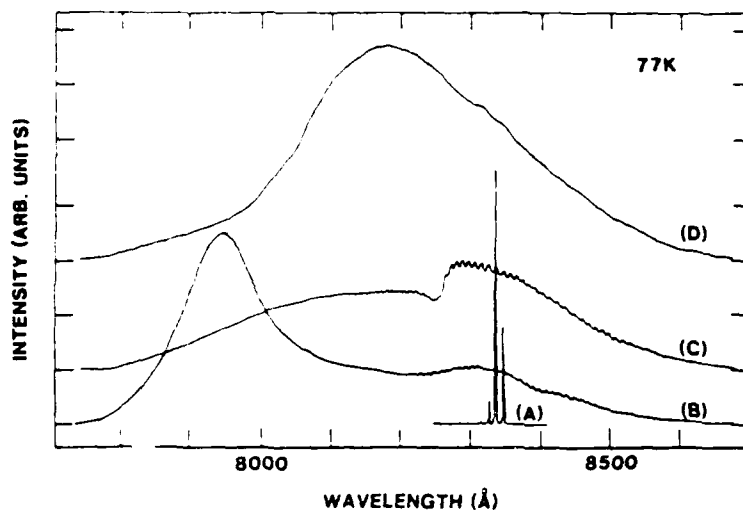


FIG. 3. (a) Laser spectrum of GaAs substrate pumped through the MQW side (80 Å GaAs/60 Å $\text{Al}_{0.5}\text{Ga}_{0.5}\text{As}$ /70 periods); (b) fluorescence spectrum of the sample used in (a) but with output coupler removed and sensitivity increased; (c) fluorescence spectrum of GaAs sample used in (a) and (b) but MQW side facing the high reflective mirror; (d) Fluorescence spectrum of a sample where the MQW was removed by selective etching.

mW. The power conversion efficiency is about 1% between 1 and 5 mW with a $R = 0.90$ output coupler and 0.4% when a $R = 0.97$ mirror was used. The threshold pump power was around 120 mW for the 90% output couplers and 80 mW for the 97% mirror. However, a precise measurement of the threshold was not possible because of its strong dependence on the pumped spot. Furthermore, we often found that lasing spots were isolated on the sample such that lasing happened to stop after shifting the sample a few microns. Despite the relatively low efficiency due to the 20% intracavity loss of the microscope objective, the achieved powers are much higher than those of other optically pumped GaAs lasers.^{6,10} Using doublet lenses (Melles Griot 06LAI) designed and AR coated for work with diode lasers at 830 nm, failed to achieve any lasing, indicating that a well corrected optical system is more important than using lenses with minimum transmission loss. However, microscope objectives specially designed for intracavity use at the laser wavelength should result in much higher output powers.

The pulse width of the laser was determined with an autocorrelator to be 18 ps (FWHM) assuming single-sided exponential pulses. This measurement correlates with the obtained spectral data of the laser linewidth of 1.5 Å, resulting in a time-bandwidth product of 1.16. Thus, the Fabry-Perot étalon formed by the GaAs itself reduces the laser bandwidth too much to produce pulses shorter than 10 ps. Using AR coated platelets which removes the étalon effect leads to an increased bandwidth and pulses as short as 7 ps should be achievable.⁶ Additionally, single mode operation as well as fine wavelength tuning with prisms or Lyot filters would be possible.

Wavelength tuning between 8350 and 8650 Å has been accomplished by a controlled setting of the temperature between 77 and 160 K. No lasing occurred at temperatures higher than 160 K. The observed wavelength shift of about 3 Å/K is in good agreement with¹¹ but about twice of that found for the CdS lasers.¹

In conclusion, we have demonstrated the first mode

locking of Si-doped bulk GaAs platelets producing 18 ps pulses with peak powers of up to 3.3 W. AR coating of the crystals may yield a larger intracavity bandwidth and thus even shorter pulses. Furthermore, using GaAs platelets grown by liquid phase epitaxy or similar techniques, having greatly reduced impurity concentration compared to the substrates used, should lead to a better controlled laser wavelength characteristic and cw operation. The GaAs laser fills a gap in the row of synchronously pumped semiconductor lasers in the important wavelength interval between 800 and 900 nm. With our pumping scheme a very good beam quality could be achieved which is one of the great advantages over all other GaAs lasers. In addition, other doped semiconductor materials can be used for extended tunable picosecond pulse generation throughout the visible and near infrared.

The authors gratefully acknowledge the preliminary studies of J. M. Costa and the technical assistance of D. J. Olson. This work was supported by the U.S. Army Research Office.

¹C. B. Roxlo, D. Bebelaar, and M. M. Salour, *Appl. Phys. Lett.* **38**, 507 (1981).

²C. B. Roxlo and M. M. Salour, *Appl. Phys. Lett.* **38**, 738 (1981).

³R. S. Putnam, C. B. Roxlo, M. M. Salour, S. H. Groves, and M. C. Plonko, *Appl. Phys. Lett.* **40**, 660 (1982).

⁴R. S. Putnam, M. M. Salour, and T. C. Harman, *Appl. Phys. Lett.* **43**, 408 (1983).

⁵R. S. Putnam and M. M. Salour, *Proceedings of the SPIE (Society of Photo-Optical Instrumentation Engineers)*, **439**, 66 (1984).

⁶W. L. Cao, A. M. Vacher, and C. H. Lee, *Appl. Phys. Lett.* **38**, 653 (1981).

⁷J. P. Van der Ziel, in *Semiconductors and Semimetals*, Vol. 22, Part B, Lightwave Communications Technology, edited by W. T. Tsang (Academic, Orlando, Florida, 1985), Chap. 1.

⁸D. C. Reynolds, K. K. Bajaj, C. W. Litton, P. W. Yu, W. T. Masselink, R. Fischer, and H. Morkoç, *Phys. Rev. B* **29**, 7038 (1984).

⁹W. T. Masselink, P. J. Pearah, J. Klem, C. K. Peng, H. Morkoç, G. D. Sanders, and Y. C. Chang, *Phys. Rev. B* **32**, 8027 (1985).

¹⁰S. R. Chinn, J. A. Rossi, C. M. Wolfe, and A. Mooradian, *IEEE Quantum Electron. QE-9*, 294 (1973).

¹¹R. C. Miller, R. Dingle, A. C. Gossard, R. A. Logan, W. A. Nordland, and W. Wiegman, *J. Appl. Phys.* **47**, 4509 (1976).

3-ps compressed pulses from a mode-locked Kr⁺ laser

B. Vaik, K. Vilhelmsson, and M. M. Salour

T-4C4N Aerospace Corporation, 2111 Palomar Airport Road, Carlsbad, California 92008

(Received 11 December 1986; accepted for publication 12 January 1987)

We report on 33× compression of 100-ps mode-locked Kr⁺ laser pulses at 647.1 nm by using a fiber-grating-pair compressor. Pulses with very low wings have been achieved by making use of the nonlinear birefringence effect leading to an intensity-dependent state of polarization. The discrimination of the wings took place in the grating compressor which acted as a polarizer.

Optical pulse compression by means of a single-mode fiber in conjunction with a grating-pair compressor has become a very powerful technique to achieve ultrashort pulses with mode-locked dye lasers.^{1,2} Optimal conditions for the application of this method, concerning fiber length and grating separation, are found for initial pulse durations on the order of some picoseconds.¹ However, effective pulse compression of relatively long pulses (80–100 ps) has been demonstrated recently with mode-locked Nd:YAG lasers at 1.06 μm ^{3,4} and at 1.32 μm .⁵ To our knowledge, the longest reported pulses which have been compressed in the visible region were 33 ps from a mode-locked and frequency-doubled Nd:YAG laser at 0.532 μm .⁶

In this letter we report on 33 times compression of mode-locked Kr⁺ laser pulses at 647.1 nm from 100 ps down to 3 ps. Furthermore, by taking advantage of the nonlinear birefringence effect in the fiber in conjunction with the polarization-dependent transmission of the grating pair, we obtained compressed pulses with very low wings. This method of wing reduction has been applied successfully for soliton-like subpicosecond pulses,⁷ for reshaping of 3 ps pulses,¹⁰ and in conjunction with a pulse compressor generating subpicosecond pulses.¹¹ The phase shift of each polarization, accumulated by the field components along each of the two principal axes of a fiber, is generally different leading to an elliptical output polarization. It can be linearized by means of a quarter-wave plate or Soleil-Babinet compensator. However, at high peak powers, the polarization becomes intensity dependent and is not the same at the peak of the pulse as in the lower intensity wings. With appropriate polarizers, it is therefore possible to separate these wings from the compressed pulse.

The experimental arrangement is shown in Fig. 1. A mode-locked Kr⁺ laser (Spectra Physics 171) emits 100-ps pulses at 647.1 nm with a repetition rate of 82 MHz. The average power of the laser was 1.2 W. An acousto-optic modulator was used as a variable attenuator and to isolate the laser from backreflected light, which was detrimental for the mode locking. With a 20× objective the light was coupled into a 60-m-long single-mode fiber (Lightwave Technology F1506E) having a fused silica core of 3.6 μm diameter. The attenuation of the fiber at 633 nm was 10.8 dB/km and, taking into account all reflection losses as well as a typical coupling efficiency of >75%, the overall transmission was 52%. At this point we would like to emphasize the importance of using pure silica core fibers for visible light instead of the more easily available germanium doped core

fibers. The latter did not withstand the high peak powers over more than a few hours. After that time we observed a strong increase in attenuation which previously has been attributed to the generation of color centers.¹²

With a half-wave plate before the fiber, the orientation of the linear input polarization could be rotated with respect to the principal axes of the fiber. The output polarization could be changed by means of a quarter-wave plate and rotated for maximum transmission through the grating compressor with an additional half-wave plate. The compressor assembly, consisting of two holographic gratings with 2400 l/mm, was used in double-pass configuration producing a round output beam. The gratings were used near Littrow condition with 44° and 57° for the incident and the diffracted beam, respectively. The reflectivity for the s

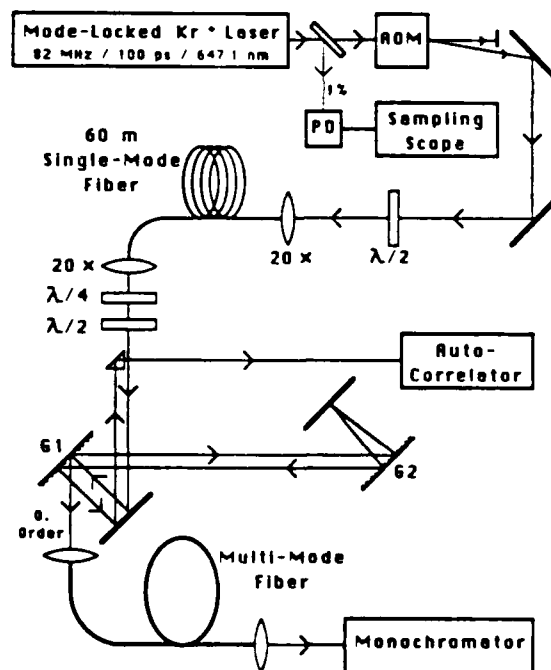


FIG. 1. Experimental setup. AOM is an acousto-optic modulator, PD is an ultrafast photodiode, and G_1 and G_2 are gratings with 2400 l/mm.

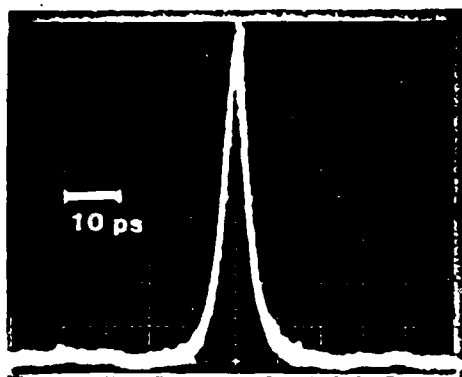


FIG. 2. Autocorrelation trace of the compressed pulses with a width of about 5 ps (10 scans). The calculated pulse width is 3 ps assuming sech² pulse shape. Zero intensity is at the bottom of the grid.

and *p* polarization was $R_s = 0.65$ and $R_p = 0.1$ (*p* polarization is parallel to the grooves) resulting in a total double-pass transmission through the grating pair of $T_t = 0.18$ and a negligible transmission for the orthogonal polarization. For compressed pulses of high quality, the typical transmission of the total fiber-grating-pair compressor was about 5%. This relatively low transmission can be increased by a factor of 2–3 by using gratings with a higher reflectivity and by operating it in single-pass configuration with appropriate beam-shaping optics.

An autocorrelation trace of the compressed pulses is shown in Fig. 2. Assuming a sech² shape, the pulse width is 3 ps which corresponds to a compression factor of 33. The average input power was about 1 W and the distance between the gratings was 1.88 m, corresponding to a compressor length of $b = 3.76$ m. A fine adjustment of the compressor length was not necessary because a slight change of the input power was sufficient to match the peak power in the fiber to the optimal compressor length. The measured average power after the compressor was 47 mW which corresponds to a peak power of about 180 W.

To generate pulses with low wings, as shown in Fig. 2, the orientation of the input and output polarization, with respect to the fiber axis and grating pair, was adjusted carefully with the help of the autocorrelation signal. After launching maximum power into the fiber and tuning the half-wave plate after the fiber to maximum transmission through the compressor, rotation of the wave plate at the input and a slight reduction of the input power always resulted in compressed pulses with more or less pronounced wings. Final wing reduction and shortest pulses were then achieved by successively changing the orientation of the input and output half-wave plate along with the quarter-wave plate.¹³ Rotation of the input polarization by 90° together with a readjustment of the wave plates after the fiber resulted in the same pulse shape. At angles between these two orientations, the compressed pulses exhibited various pedestals, wings, and sidelobes or the compression was poor.

In addition to the wing clipping method described above, we tried spectral windowing.¹⁴ It was possible to ob-

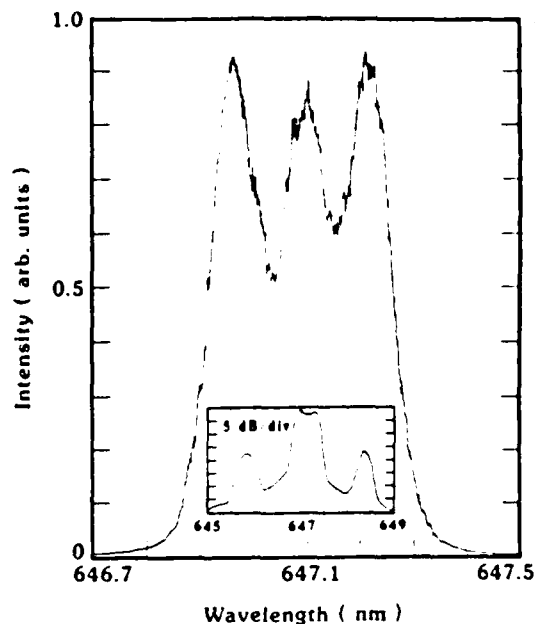


FIG. 3. Spectrum emitted from the fiber. The average power before the fiber is 1 W and the output power is 0.52 W (0.05 nm resolution). A logarithmic plot of the spectrum after the fiber (different angle of input polarization), illustrating the distinct sidelobes, is shown in the inset.

tain smooth Gaussian-shaped 7-ps pulses without wings; however, the average power after the compressor dropped to below 1 mW. Therefore, it seems not preferable to use spectral windowing in conjunction with nonpolarization preserving fibers exhibiting nonlinear birefringence.

The spectrum of the pulses after transmission through the fiber is shown in Fig. 3. Assuming bandwidth-limited 100-ps Gaussian pulses from the Kr⁺ laser, the initial linewidth is 0.0074 nm (FW1/e). The measured width of the spectrum was 0.39 nm corresponding to a spectral broadening by a factor of 53. Additionally, we observed distinct sidelobes in the spectrum (insert Fig. 3). Their formation was dependent on the input polarization, and they could be produced repetitively by 45° rotations of the half-wave plate before the fiber. The polarization of the light in the sidelobes was different from that in the central part of the spectrum leading to their suppression in the grating-pair compressor. In a recent paper,¹⁵ such sidelobes were interpreted as optical wave breaking occurring in fibers which are long enough for group velocity dispersion to act on the temporal shape of the pulse. Their generation in our experiment was surprising, since the ratio z/z_c was about a factor of 10 smaller and the normalized amplitude A larger by a factor of 1.5 than that used for calculations in Ref. 15. A detailed analysis would lie beyond the scope of this letter and is subject to future investigation. In contrast to other pulse compression experiments with long input pulses, we experienced no limitation by stimulated Raman scattering which was always less than 1%.

For a comparison of our results with theory, we use the

definitions given in Refs. 3 and 16. For $0.647\text{ }\mu\text{m}$ and 100 ps the normalized length is $z_0 = 100\text{ km}$ ($C_1 = 0.1\text{ m}^{-1}\text{ ps}^2$). The maximum phase shift $\Delta\phi$ accumulated in a fiber is given by $\Delta\phi = k z n_2 I$ with $k = 2\pi/\lambda$ and $n_2 = 3.2 \times 10^{-16}\text{ cm}^2/\text{W}$, z equals the fiber length, and I is the peak intensity. This phase shift is related to the width $\partial\omega$ of the broadened spectrum and the initial linewidth $\Delta\omega_0$ (both FWHM) of bandwidth-limited Gaussian pulses by⁹ $\Delta\phi = 1.16\partial\omega/\Delta\omega_0$ and can be determined spectroscopically. $\Delta\phi$ is related to the normalized amplitude A from Ref. 3 by $\Delta\phi = \pi/2 A^2/z_0$. Hence, for $z \ll z_0$, the compression ratio can be expressed by $t_0/t = 1 + 0.57\Delta\phi$ and the grating separation is $b = 0.13\pi C_2 t_0^2/2\Delta\phi$ ($C_2 = 0.133$ for 2400 l/mm and a diffraction angle of 57° , b is in meters and t_0 is in picoseconds). The 53 times spectral broadening ($\Delta\phi = 61.5$) results in a compression ratio of $t_0/t = 36$ and a grating separation of $b = 4.41\text{ m}$, which is in agreement with the experiment. The calculation of the grating separation and the compression ratio with the approach described above led to more reliable values than using the normalized amplitude A estimated from the peak power in the fiber.

In conclusion, we have demonstrated the possibility of effectively compressing relatively long pulses with medium peak powers in the visible spectrum to a few picoseconds using a fiber-grating-pair compressor. Additionally, we have demonstrated the feasibility of a pulse-resaping technique based on the nonlinear birefringence in fibers for long input pulses. A better peak power enhancement can be expected by using gratings with higher reflectivity or by utilizing a single-pass configuration together with beam-shaping optics. One potential application of the compressed pulses is their use as a pump source for optically pumped GaAs multiple quantum well lasers¹⁷ which should lead to the generation of sub-picosecond pulses from those lasers.

The authors would like to thank D. J. Olson and E. L. Mason for technical assistance. This work was supported by the U. S. Army Research office.

- ¹B. Nikolaus and D. Grischkowsky, *Appl. Phys. Lett.* **42**, 7 (1983); S. L. Palfrey and D. Grischkowsky, *Opt. Lett.* **10**, 562 (1985).
- ²W. H. Knox, R. L. Fork, M. C. Downer, R. H. Stolen, C. V. Shank, and J. A. Valdmanis, *Appl. Phys. Lett.* **46**, 1120 (1985).
- ³W. J. Tomlinson, R. H. Stolen, and C. V. Shank, *J. Opt. Soc. Am. B* **1**, 139 (1984).
- ⁴J. D. Kafka, B. H. Kolner, T. Baer, and D. M. Bloom, *Opt. Lett.* **9**, 505 (1984).
- ⁵A. S. L. Gomes, U. Österberg, W. Sibbett, and J. R. Taylor, *Opt. Commun.* **54**, 377 (1985).
- ⁶B. Zysset, W. Hodel, P. Beaud, and H. P. Weber, *Opt. Lett.* **11**, 156 (1986).
- ⁷K. Tai and A. Tomita, *Appl. Phys. Lett.* **48**, 309 (1986).
- ⁸A. M. Johnson, R. H. Stolen, and W. M. Simpson, *Appl. Phys. Lett.* **44**, 729 (1984).
- ⁹R. H. Stolen, J. Botineau, and A. Ashkin, *Opt. Lett.* **7**, 512 (1982).
- ¹⁰B. Nikolaus, D. Grischkowsky, and A. C. Balant, *Opt. Lett.* **8**, 189 (1983).
- ¹¹N. J. Halas and D. Grischkowsky, *Appl. Phys. Lett.* **48**, 823 (1986).
- ¹²R. H. Stolen, in *Optical Fiber Telecommunication*, edited by S. E. Miller and A. G. Chynoweth (Academic, New York, San Francisco, London, 1979), Chap. 5.
- ¹³With the help of the quarter-wave plate it was possible to increase the average power after the compressor; however, after best quality compressed pulses were achieved, the wave plate could be removed without changing the amplitude of the autocorrelation signal. This indicates that the additional power contributed mainly to the long, but low power wings.
- ¹⁴J. P. Hentage, R. N. Thurston, W. J. Tomlinson, A. M. Weiner, and R. H. Stolen, *Appl. Phys. Lett.* **47**, 87 (1985).
- ¹⁵W. J. Tomlinson, R. H. Stolen, and A. M. Johnson, *Opt. Lett.* **10**, 457 (1985).
- ¹⁶R. H. Stolen, C. V. Shank, and W. J. Tomlinson, in *Ultrafast Phenomena IV*, edited by D. H. Auston and K. B. Eiseenthal (Springer, Berlin, Heidelberg, New York, Tokyo, 1986), p. 46.
- ¹⁷B. Valk, M. M. Salour, G. Munns, and H. Morkoç, *Appl. Phys. Lett.* **49**, 549 (1986).

END

DATED

FILM

8-88

DTIC